COMPACT DNP POLARIZER FOR MRI APPLICATIONS AT 1.5 T

V. Denysenkov[1], R. Maeder[2], S. Fischer[2], M. Terekhov[3], T. Vogl[2], T. F. Prisner[1]

[1]Institute of Physical and Theoretical Chemistry, and Center for Biomolecular Magnetic Resonance, Goethe-University, Max-von-Laue Str.7, 60438 Frankfurt am Main, Germany

[2]Institute of Diagnostic and Interventional Radiology, University Hospital Frankfurt, Frankfurt am Main, Germany

[3] Comprehensive Heart Failure Center, University Hospital, Würzburg, Germany

Introduction

Magnetic Resonance Imaging (MRI) is widespread in clinical diagnostics providing information on physiological and metabolic changes in tissue *in-vivo*. Beside the wonderful features it has following limitations:

- low contrast due to low intrinsic NMR sensitivity,
- long acquisition times, resulting in artifacts caused by motion of the object.

Low contrast can be improved by a Gd-complex administration, but sometimes with side effects (5% of patients).

Dynamic nuclear polarization (DNP) of protons in water can also be used for MRI contrast improvement promising to reduce the above mentioned limitations.

In our DNP setup (Fig. 1), based on Overhauser DNP method, continuous flow of water is hyperpolarized inside the resonator under microwave excitation in presence of TEMPO molecules [1], and then administrated into the object under study, which can be a small animal like mouse. The method is promising for MRI angiography applications.

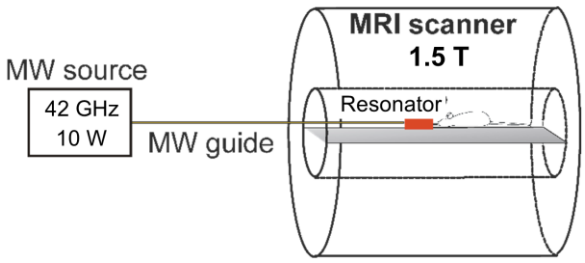

Fig. 1. In-bore MRI DNP setup. While both the imaging and the actual DNP process takes place in bore of the MRI magnet at 1.5 T, the microwave source has to be kept out of the magnetic field. Transmission of the microwave power is achieved by the WR-28 hollow waveguide, without significant power losses (1 dB) [2].

Experimental

DNP experiments are performed by tuning the resonator and the source to the resonance frequency of the radical's electron spins corresponding to the magnetic field strength at the resonator's position, which can be easily determined by performing a frequency-swept continuous wave (CW) ESR experiment. Then, the sample is pumped through the resonator while the electronic transition is saturated by continuously irradiating at said frequency, which is approximately 42 GHz for a nitroxide radical. Clearly, the resonator is also subject to the field gradients used during imaging sequences and is therefore momentarily off resonance when gradients are applied. However, since this is only the case for very short periods it does not play a significant role. our MRI scanner (Magnetom Aera 1.5 T, Siemens Erlangen Germany) microwave of 41.991 GHz was resonant with the central nitrogen (^{14}N) hyperfine line of the TEMPOL radical.

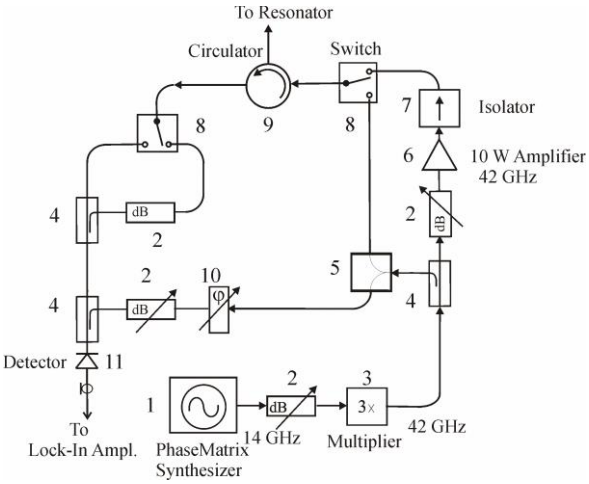

Fig. 2. The 42 GHz microwave board: (1) microwave synthesizer; (2) attenuators; (3) frequency multiplier; (4) directional couplers; (5) power divider; (6) 10 W 42 GHz amplifier; (7) isolator; (8) mechanical switches; (9) circulator; (10) phase shifter; (11) detector [4].

Figure 2 shows the block-diagram of the microwave board, which consists of a 14 GHz synthesizer (Phase Matrix, USA), a frequency Tripler (QuinStar, USA) and a 10 W 42 GHz power amplifier (QuinStar, USA). The microwave signal reflected from the resonator can be monitored after the circulator by a microwave diode detector (Spacek Labs, USA). This signal is used to detect and tune the microwave resonator and 0to determine the EPR resonance frequencies for optimum DNP excitation. The output power can be regulated manually between 0.3 W and 11 W by a calibrated attenuator.

The most important component of the in-bore DNP polarizer is the microwave resonator. It consists of a cylindrical cavity (ID 9.2 mm) made of copper exploiting the TE013 circular mode. The resonator shape with the couple waveguide and the mode pattern are shown in Fig. 4a. The reason for using the TE013 instead of TE011 mode is to increase the sample volume inside the cavity. The cavity has a length of 34 mm between both plungers

defined by the MW frequency of 42 GHz, resulting in a sample volume of 4.3 µl inside the cavity. The residence time inside the microwave cavity of the flowing water solution has to be on the order of the proton spin relaxation time (0.2 sec. for a 28 mM TEMPOL/water solution at 60 °C) to achieve optimum polarization enhancements.

Results

First experiments on a blood vessel phantom (Fig.3) demonstrate that even under dilution of the injected hyperpolarized liquid in a bloodstream of an animal, hyperpolarized signal can be obtained with our existing setup (Fig. 8). The used phantom consist of a 1 mm ID plastic tubing connected to a perfusion pump with a physiological buffer solution with 2.4 ml/min flow rate, corresponding to the aorta of a mouse. The hyperpolarized water/TEMPOL solution was injected into this stream by a 0.15 mm ID quartz capillary with a flow rate of 1.5 ml/min. Imaging in this vessel phantom featured a contrast enhancement up to a factor 5, which decreased by 50% after 3.5 cm and went back to its origin after 5 cm during dilution by the downstream

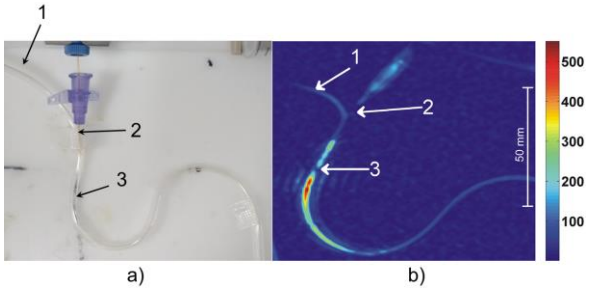

Fig. 3. (a) Phantom for injection of DNP enhanced liquid in a blood vessel: (1) 1 mm ID plastic tubing filled with 0.9% NaCl physiological buffer solution with a flow rate of 2.4 ml/min. (2) Quartz capillary with 0.15 mm ID used for the injection of 28 mM TEMPOL solution with a flow rate of 1.5 ml/min. (3) End of the injection capillary inside the phantom blood vessel. (b) The injected hyperpolarized liquid is clearly visible with enhanced contrast in the non-polarized physiological buffer flow stream.

Performance of the polarizer was tested also on mouse by injection of hyperpolarized substrate into aorta (Fig. 4a). Similar test was also accompished with Gd-chelate complex as a typical contrast agent administrated for comparison (Fig. 4b). It is clear visible better contrast in the case of DNP that is promising indication for future applications in angiography.

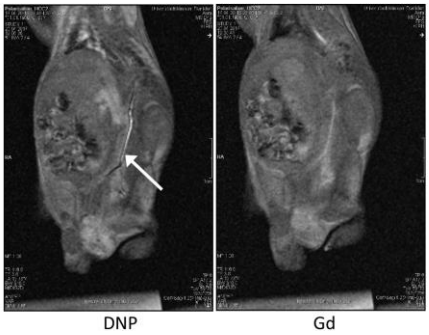

Fig. 4. (left) DNP hyperpolarized substrate administrated into aorta. Arrow (white) shows injection point; (right) Gd-contrast agent (Gadovist 1 mM/ml) administrated in aorta via the same catheter.

Conclusions

By the results achieved on phantoms, we demonstrated the performance of our in-bore DNP setup, which is capable to operate with flow rates up to 30µl/sec and local contrast enhancements up to 5-fold, which is promising for small animals experiments.

Outlook

Immobilizing the TEMPOL radical inside the microwave resonator: can help to minimize losses of enhanced signal due to the short relaxation time induced by the paramagnetic radicals.

Optimization of acquisition parameters (pulse sequences): to avoid depletion of hyperpolarization (by traditional multiple scans), that can improve the contrast enhancement.

Ackowledgements

We thank the German Research Society (DFG) for financial support

References

1. *McCarney, E.R, Armstrong, B.D., Lingwood, M. D., Han, S.* Hyperpolarized water as authentic magnetic resonance imaging contrast agent // Proc. Nat. Acad. Sci. 2007. V. 104, P. 1754–1759.

2. *Krummenacker, J., Denysenkov, V., Terekhov, M., Schreiber, L., Prisner, T.* DNP in MRI: An in-bore approach at 1.5T // J. Magn. Reson. 2012. V. 215, P. 94-99.

3. *Terekhov, M., Krummenacker, J., Denysenkov, V., Gerz, K., Prisner, T., Schreiber, L.* Inversion-recovery preparation for improving the visualization of continuous flow Overhauser DNP hyperpolarized water // Magn. Reson. Med. 2015. V. 75, P. 985–996.

4. *Denysenkov, V., Terekhov, M., Maeder, R., Fischer, S., Zangos, S., Vogl, T., Prisner, T.* Continuous-flow DNP polarizer for MRI applications at 1.5 T // Sci. Rep. 2017. V. 7, P. 44010.

Overhauser DNP applications at 9.4 Tesla by using terahertz irradiation

V. Denysenkov [1], O. Jakdetchai[2], J. Becker-Baldus[2], C. Glaubitz[2], T. Orlando[3], M. Bennati[3], T. Prisner[1]

[1]Institute of Physical and Theoretical Chemistry, Center for Biomolecular Magnetic Resonance, Goethe University, Frankfurt am Main, Germany
[2]Institute of Biophysical Chemistry, Center for Biomolecular Magnetic Resonance, Goethe University, Frankfurt am Main, Germany
[3]ESR Spectroscopy Group, Max Planck Institute, for Biophysical Chemistry, Göttingen, [3] Germany

Dynamic nuclear polarization (DNP) is a well known method that helps to increase amplitude of nuclear magnetic resonance (NMR) signals [1]. Here we present results of study of different biological compounds such as lipid multilayers, diethyl malonate, and ethyl-acetoacetate by ^{1}H DNP, and ^{13}C DNP at 9.4 Tesla [4, 5]. Continuous wave irradiation of a 263 GHz gyrotron (GYCOM) has been applied to pump electron spin transitions in 4-Oxo-2,2,6,6-tetramethylpyperidine, which has been used as a source of unpaired electron spins. Experiments were carried out at 263 GHz electron paramagnetic resonance (EPR) frequency and 400 MHz NMR proton frequency by using a stripline structure combined with a Fabry−Perot microwave (MW) resonator, in the case of aligned bilayers, and at 263 GHz/100 MHz NMR ^{13}C frequency by using a helix double resonance structure, in the case of small organic molecules. Here we demonstrate as a proof of concept that a significant NMR signal increase (15-fold for lipids, and 13- 30-fold for the small organic molecules) under ambient conditions can be achieved by utilizing the Overhauser DNP effect. Our results demonstrate that Overhauser DNP at high fields provides efficient polarization transfer from electron spins to nuclei within the biological samples, which is driven by fast local molecular fluctuations at ambient temperatures.

Introduction

Recently very high NMR signal enhancements up to a factor of 1000 could be observed by applying DNP in liquids at high magnetic fields [3]. In this paper, we describe experimental requirements to perform Overhauser DNP at high magnetic fields. For the excitation of the EPR transitions at high magnetic fields (3-23 Tesla), MW in the range of 100 GHz - 1 THz is required. To avoid strong absorption of the THz radiation by liquids, resonant structures with spatial separation of the electrical and magnetic components of the MW are necessary. Such double resonant (NMR and EPR) structures, working at high magnetic fields, will be described in this paper. The MW resonant structure limits the sample dimension much below the MW wavelength, strongly decreasing the overall sample amount accessible for liquid DNP experiments at high magnetic fields. The field dependence of all factors influencing the Overhauser DNP efficiency and the overall NMR signal-to-noise improvement will be also discussed.

In the case of Overhauser DNP the change of the electron spin magnetization S_z is determined by its fast intrinsic relaxation rate R_{1S} and its interaction with the MW excitation, described by the MW field strength in radian frequency units □□ (Figure 1).

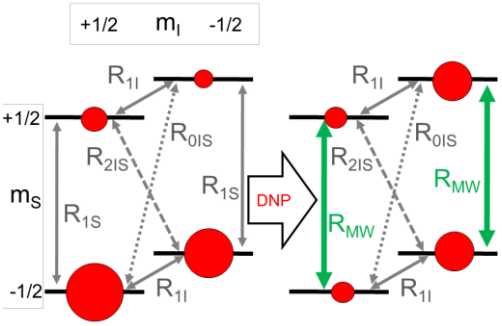

Fig. 1. Energy level diagram for a coupled electron spin S=½ and nuclear spin I=½. Left side: Populations at thermal equilibrium with relaxation rates between the levels. Right side: Changed populations of the levels if the allowed electron spin transitions are saturated by the microwave excitation, resulting in an enhanced nuclear spin polarization.

Experimental

One of the first resonance structures used in our DNP experiments is the helix double resonance structure (Fig. 2) featured in a high (5 G/W$^{1/2}$) MW conversion factor and small volume of the liquid sample (4 nl). The resonance structure is a cylindrical TE011 cavity, where the cylinder is made of a copper tape forming a helical six-turn coil used for RF excitation/detection at NMR frequency. Placing the sample along the resonator axis, in the node of the electrical field component in the MW cavity allows to reduce strongly the absorption and thus heating, while the MW magnetic field component, necessary to excite the electron spin transitions, is maximum at the sample position and strongly enhanced by the resonator Q value [2].

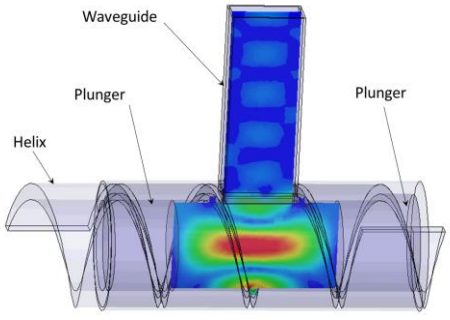

Fig. 2. Helical resonance structure operating TE011 circular mode at 263 GHz: contour plot of microwave B field distribution.

Another double resonance structure developed in Frankfurt is shown in Fig. 3. It is a combination of a stripline and a semi confocal Fabry-Perot resonator. The stripline is tuned to NMR frequency of 400 MHz, and the Fabry-Perot is tuned to EPR frequency of 263 GHz.

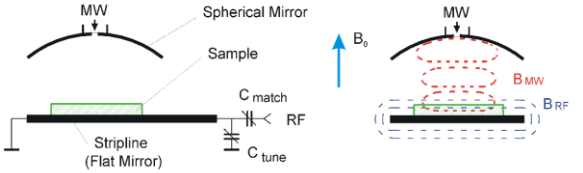

Fig. 3. Stripline-Fabry-Perot resonance structure operating at RF = 400 MHz and at MW = 263 GHz.

DNP results

With the helix resonance structure.

NMR signal enhancements were quantified by comparing signal integrals of spectra acquired with and without microwave, as previously described. Due to resonator construction, part of the sample is located outside the resonator, but still within the NMR coil detection range. For this reason, Boltzmann thermal equilibrium spectra display a second signal about 2 to 4 ppm apart from the reference and that is not enhanced with DNP. Such peaks are labelled with an asterisk and not considered in data analysis [5].

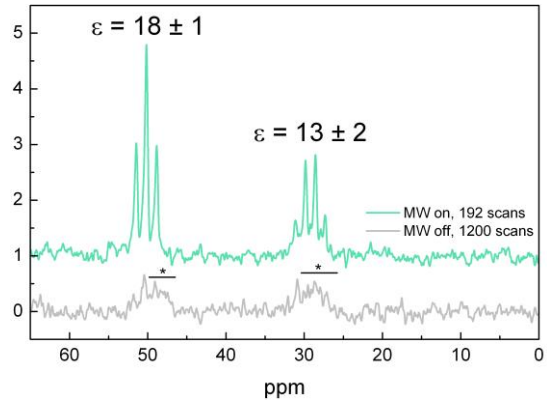

Fig. 4. DNP enhancements in ^{13}C-2-4-ethyl acetoacetate (recycle delay 10 s) [5].

With the Fabry-Perot resonance structure:

Our Fabry-Pérot resonator for MW excitation at 260 GHz described above can accommodate 90 nl of a disc-shaped sample within about 3 mm diameter. This is an ideal geometry for partially aligned multi-layers of lipid bilayers. Several layers of lipid bilayers 1,2-dioleoyl-*sn*-glycero-3-phosphocholine (DOPC) doped with nitroxide radicals and exposed to water were mechanically deposited directly onto the surface of the flat mirror with a total thickness of approximately 20 μm (approximately 2000 bilayers, 160 μg). This assures that the wet lipid layers are situated in the maximum of the MW magnetic field and at a minimum of the MW electrical field component. The low main phase transition temperature of DOPC of -17°C ensures that the sample is in the fluid phase at room temperature. For NMR detection of the lipid proton signal, the flat mirror of the Fabry-Pérot resonator serves as a stripline RF probe tuned to 400 MHz (proton spin Larmor frequency) (Fig. 5).

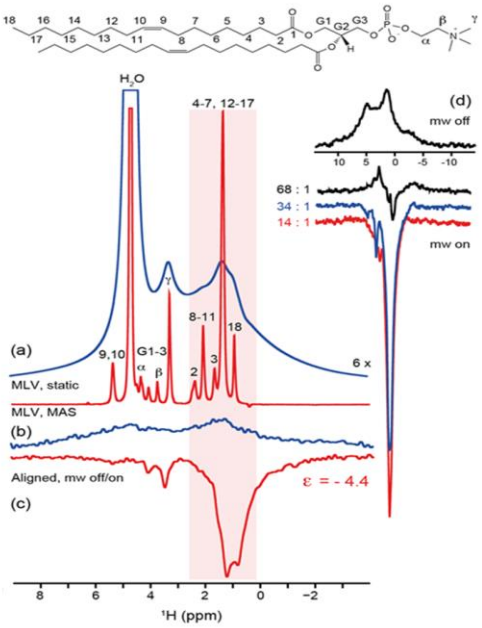

Fig. 5. ^{1}H NMR spectra of DOPC vesicles (static and MAS at 600 MHz). (b) ^{1}H NMR spectrum of DOPC doped with TEMPOL (DOPC:TEMPOL 34:1) and hydrated with D_2O (DOPC:D_2O 1:27) (c) Upon microwave irradiation (5.6 W), an enhancement of -4.4 was observed for the acyl chain proton resonances. (d) The enhancement increases with the amount of TEMPOL present [4].

References

1. *Griesinger, C., Bennati, M., Vieth, H.M., Luchinat, C., Parigi, G., Höfer, P., Engelke, F., Glaser, S.J., Denysenkov, V., Prisner, T.F.* Dynamic nuclear polarization at high magnetic fields in liquids // Prog. Nuc. Mag. Res. Spec. 2012. V. 64. P. 4-28.

2. *Denysenkov, V., Prandolini, M., Krahn, A., Gafurov, M., Endeward, B., Prisner, T.F.* High-field DNP spectrometer for liquids // Appl. Magn. Reson. 2008. V. 34. P. 289-299.

3. *Liu, G., Levien, M., Karschin, N., Parigi, G., Luchinat C., Bennati, M.* One-thousand-fold enhancement of high field liquid nuclear magnetic resonance signals at room temperature // Nature Chemistry, 2017. V. 9. P. 676-680.

4. *Jakdetchai, O., Denysenkov, V., Becker-Baldus, J., Dutagaci, B., Prisner, T., Glaubitz, C.* Dynamic nuclear polarization-enhanced NMR on aligned lipid bilayers at ambient temperature // J. Am. Chem. Soc. 2014. V. 136. P. 15533–15536.

5. *Orlando, T., Dervisoglu, R., Levien, M., Tkach, I., Prisner, T., Andreas, L., Denysenkov, V., Bennati, M.* Hyperpolarization of 13C Nuclear Magnetic Resonance Signals in the Liquid-State // Nat. Com, (submitted).

Study of PVC-based Skin Phantom with graphite particles in Terahertz Frequency Range

T. Zhang[1], M. K. Khodzitsky[1], P. S. Demchenko[1],
A. V. Bykov[1,2], A. P. Popov[1,2] and I. V. Meglinski[1,2]

[1]Terahertz Biomedicine Laboratory, ITMO University, Saint Petersburg, Russia, tmzhang91@gmail.com
[2]Biophotonics Group, University of Oulu, Oulu, Finland

1. Introduction

The development of any optical imaging system requires the use of tissue-simulating objects (phantoms) to mimic human or animal tissues for device calibration. Calibration procedures need stable materials with accurately controlled optical properties. However, such a beneficial combination is hardly possible for real biological tissues and organs: due to extraction from their natural environment their properties change over time. Therefore, the phantoms being the substitutes for real biological objects are in high demand.

Many types of phantoms have been developed for THz technology in early studies. For the breast cancer, phantoms that were composed of water, oil, surfactant TX151, agar, nano-diamonds and nano-onions in varying proportions have been designed to represent the optical properties of breast tissue in THz frequency range [1], as well as the phantoms that were composed of water, lipid and collagen [2]. Using over-the-counter soft contact as a phantom of cornea has been reported in article [3]. The phantom that is made by porcine derived gelatin with water content from 83% to 95% was tested in article [4]. All these phantoms are hydrated phantoms due to their certain water content.

Since THz radiation is very sensitive to the presence of water, and water evaporation affecting the measurement, a water-free phantom needs to be developed for stable and constant usage. One of the popular and established approaches for tissue phantom manufacturing utilizes PVC as a matrix material [5]. These phantoms possess high flexibility, elasticity and serve as optical analogues of biotissue in visible and NIR spectral regions. In this article, a PVC-based, water-free phantoms to mimic human skin in THz frequency range was examined for the first time to our knowledge.

2. Sample Preparation

The proposed phantoms were originally designed for the optical and NIR spectral range and used for research in the field of optical coherence tomography (OCT) [5]. It was made using a scattering agent and a matrix material. The scattering agent was chosen to be zinc oxide (ZnO) nanoparticles with an average diameter of 0.35 μm at a concentration of 12 mg/ml to generate desired optical properties. A polyvinyl chloride-plastisol (PVCP) was used as a matrix material for fabrication. Some graphite was also added into the mixture to achieve enough absorbance. PVCP, graphite and ZnO nanoparticles were first mixed with each other. After sonication for 15 min, the mixture was then poured into a rectangular aluminum mold and put into an oven (180 °C) for 30 min. Finally, after cooling, the fabricated phantom is stored between glass slides to prevent PVC penetration into the plastic Petry dish [5]. Four phantoms with different graphite concentrations (10%, 12.5%, 16.7% 21.9%) were produced.

3. Experiment Setup and Signal Processing

To see, whether the phantom can be used as a proper replacement of human skin for medical research in the THz frequency range, the THz optical properties of the phantom should be assessed. Terahertz time-domain spectroscopy (THz-TDS) was used for this purpose. It is the most in-use THz device to measure sample's optical properties in the THz frequency domain [6]. It measures both the amplitude and phase of the THz pulse that is reflected by the sample or transmits through the sample [6]. With the help of Fourier transform, optical properties, such as refractive index, absorption coefficient and/or transmission coefficient can be finally obtained [6,7].

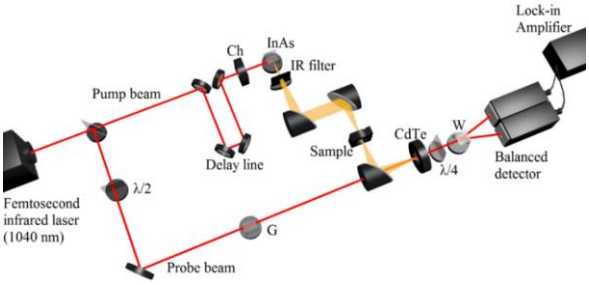

Fig. 2. The experimental setup of THz TDS system. λ/2 – half-wave plate, G - Glan prism, Ch - chopper, λ/4 - quarter-wave plate, W – Wollaston prism

The following formulas were used to calculate the refractive index and absorption coefficient basing on the spectrums and the phases we got from the fast Fourier transform (FFT) [6,7]:

$$\alpha(\nu) = -2\ln[\frac{T(\nu)E_{sample}(\nu)}{E_{reference}(\nu)}]/d \quad (1)$$

$$n(\nu) = 1 + c[\phi_{sample}(\nu) - \phi_{reference(\nu)}]/[2\pi\nu d] \quad (2)$$

$$T(\nu) = 1 - R = -[n(\nu) - 1]^2/[n(\nu) + 1]^2 \quad (3)$$

where α - the absorption coefficient, n - the refractive index of the sample, E and ϕ - the amplitude and the phase of the signal, d - the thickness of the sample, T - the Fresnel loss at the air-sample interface.

4. Results

After the calculation using formula (1) and (2), the refractive index and absorption coefficients of the phantoms were obtained and compared with the published data [8].

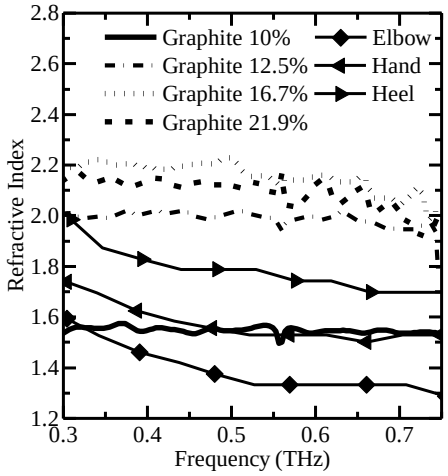

Fig. 3. Comparison of the refractive indices between phantom, elbow, hand and heel skin.

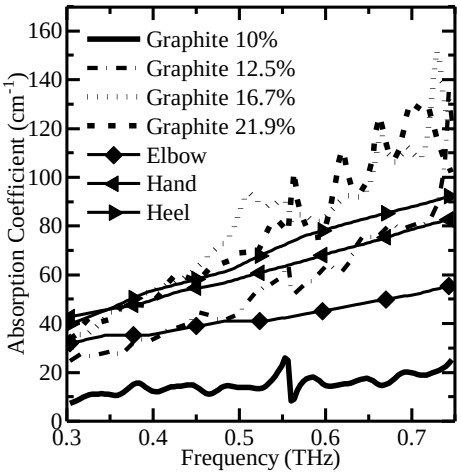

Fig. 4. Comparison of the absorption coefficients between phantom, elbow, hand and heel skin.

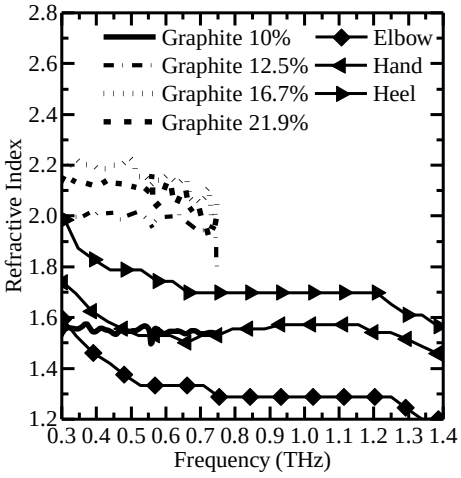

Fig. 5. Comparison of the refractive indices between phantom, elbow, hand and heel skin in a wider frequency range

Fig. 3 and Fig. 4 demonstrate the optical properties of the PVC-based phantom with graphite. The concentration of graphite influences on both refractive index and absorption coefficient of phantom. The higher the graphite concentration, the higher the value of optical properties. However, the influence of the graphite concentration also has a limit. The optical property differences between the graphite concentration of 16.7% and 21.9% are very small.

The refractive index of the phantom with 10% graphite shows good correspondence with the refractive index of hand skin in the frequency range of 0.45-0.75 THz. Fig.5 presents a good promise that in higher frequency range (>0.75THz) the phantom with 10% graphite may continue mimicking the refractive index of hand skin, since both refractive indices are nearly constant. Nonetheless, the absorption coefficient of PVC-based phantom with 10% graphite is much lower than that of any skin. The phantoms with 16.7% and 21.9% graphite possesses similar absorption coefficient as hand and heel skin in lower frequency range (0.3-0.5THz). The absorption coefficient of the phantom with 12.5% graphite is close to that of hand skin in higher frequency range (0.6-0.75THz).

5. Summary

The result proves that the presented phantoms with ZnO nanoparticles and graphite may achieve similar optical properties as human skin. The influence of different concentrations of graphites on the optical properties is also revealed. Such characteristic gives a good promise that by choosing proper concentrations of graphite, we may achieve an ideal phantom that can mimic the optical properties of human skin. Since the phantom is water-free, it can be preserved much longer than the phantom with water or lipid while the optical properties of the phantom still maintain.

Reference

1. *Bowman, T., Walter, A., et al.* phantom study of terahertz spectroscopy and imaging of micro-and nano-diamonds and nano-onions as contrast agents for breast cancer // Biomed Phys Eng Express. 2007. V. 3, No. 5. P. 055001.

2. *Truong, B.C.Q., Fitzgerald, A.J., et al.* Concentration analysis of breast tissue phantoms with terahertz spectroscopy // Biomed. Opt. Exp. 2018. V. 9. No. 3. P. 1334-1349.

3. *Sung, S., Garritano, J., et al.* Preliminary results of non-contact THz imaging of cornea // Proc. SPIE V. 9362. P. 93620C-1.

4. *Bajwa, N., Garritano, J., et al.* Reflective terahertz (THz) imaging: system calibration using hydration phantoms // Proc. SPIE. 2013. V. 8585, P. 85850W.

5. *Wróbel, M. S., Popov, A. P., et al.* Measurements of fundamental properties of human skin phantoms // J. Biomed. Opt., 2015. V. 20. No. 4. P. 045004.

6. *Dexheimer, S. L.* Terahertz Spectroscopy: Principles and Applications // CRC Press. 2007.

7. *Yasuda, H.* Measurement of terahertz refractive index of metal with terahertz time-domain spectroscopy // Jpn. J. Appl. Phys. 2008. V. 47. No. 3R. P. 1632-1634.

8. *Zaytsev, K. I., Gavdush, A. A., et al.* Highly accurate in vivo terahertz spectroscopy of healthy skin: variation of refractive index and absorption coefficient along the human body // IEEE Trans. THz Sci. Technol. 2015. V. 5. No. 5. P. 817-827

Application of high resolution subTHz spectroscopy methods for analysing the content of grain odors

V.A. Anfertev[1], V. L. Vaks[1], M.B. Chernyaeva[1], E.G. Domracheva[1], A.A. Gavrilova[2], E.V. Dabakhova[2]

[1]IPM RAS, Nizhny Novgorod, Russia, anfertev@ipmras.ru
[2]NNSAA, Nizhny Novgorod, Russia

Terahertz high resolution transient spectroscopy on nonstationary effects (free damping polarization realizing in two modes – phase switching of radiation influenced on gas and fast frequency sweeping) and spectrometers, based on these methods (a wideband spectrometer, a marker detector for registering certain gases, a two-channel spectrometer with two independent radiation sources and one detector) are very interesting for analysis of multicomponent gas mixtures.[1] The possibility of use of terahertz high resolution transient spectroscopy in such agricultural (diagnostics of degree of corn mycosis based on analysis of corn odors), medical applications (veterinary diagnostics of diseases and pathology states of animals based on analysis of exhaled breath and vapors of biological liquids (urine, saliva)); monitoring the quality of foodstuff (meat, fish, poultry) based on analysis of its odors shows considerable promise.

In this work possibility of use of terahertz high resolution transient spectroscopy in such agricultural applications as analysis of corn odors for developing the methods of quality control and diagnostics is considered. The method was used to study "odors" of grain of new unique varieties: spring wheat "Sitara", winter wheat "Nemchinivskaya-17", barley "Binom" and oats "Arkhat". Researches of "odors" of different variety of grain were provided with subTHz transient backward wave oscillator based spectrometer in frequency range of 115-160 GHz which developed in IPM RAS. THz gas transient spectrometers based on transient gas absorption effects under radiation, which comes into resonance with molecular two-level quantum system in a shorter time than in the times of relaxation processes and transition radiation, when the radiation leaves resonance in a shorter time than in the relaxation times. The spectrometer has 1kHz frequency resolution and high frequency stability of radiation (1e-8). Quartz cell length of 1 meter was used as measurement volume. Grain (whole or ground) was placed in a flask, which was connected to a measuring gas cell. The cell was pumped to operating pressure with a vacuum pumping station «Pfeiffer Hi-Cube Eco 80» to avoid unwanted gases and gas collisional broadening. For dehydration of the grain sample, vacuum drying with heating of the sample was carried out for some time. According to the developed measurement procedure, it is considered that to exclude the effect of water vapor on detecting trace concentrations of the mixture components, the pressure in the cell should be 1×10e-3÷5×10e-3 mbar. After that, the heating of the flask containing the sample of grain continues.

The preliminary results on studying the grain odors composition of wheats, barley (Binom) and oats (Arkhat) are presented in the Table 1.

Grain	Substances
Winter wheat "Nemchinovskaya-17"	Glycolaldehyde (HCOCH2OH)
	Formic acid (HCOOH)
Summer wheat (Sitara)	Formamide (NH2CHO)
barley (Binom)	Acetaldehyde (CH3CHO)
oats (Arkhat)	HCOCH2OH
	Ga-n-C3H7OH
	Acetaldehyde (CH3CHO)
	CH2(OH)-CH2-CH2(OH) Propane-1,3-diol
	CH2(OH)-CH(OH)-CH3 Propane-1,2-diol

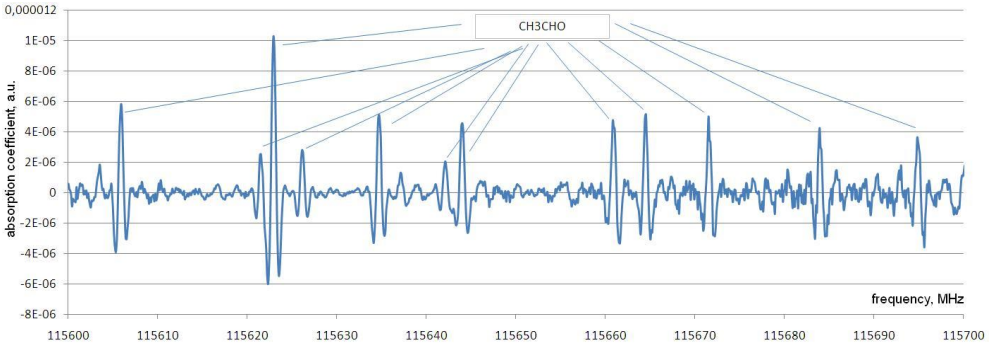

Fig. 1. The record of subTHz absorption spectrum in odor of barley ("Binom") sample after heating

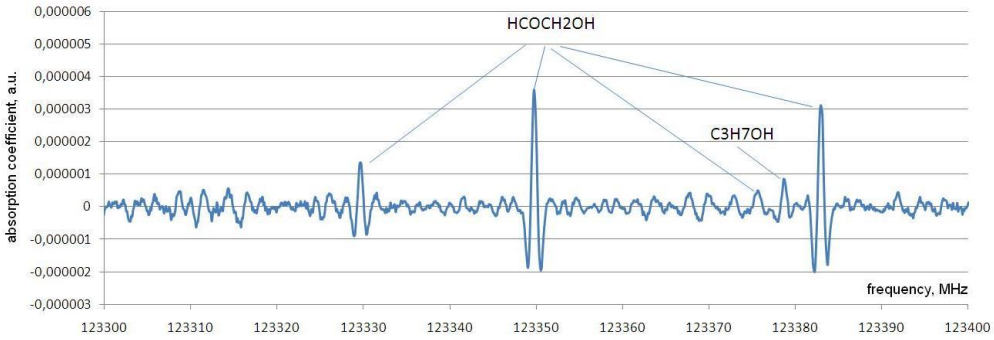

Fig. 2. The record of subTHz absorption spectrum in odor of oats ("Arkhat") sample after heating

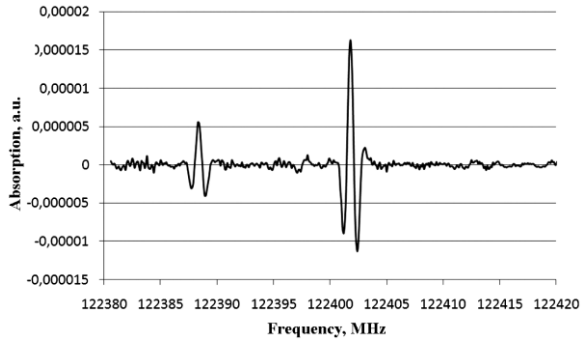

Fig. 3 The record of subTHz absorption spectrum of formamid in "odor" of summer wheat "Sitara"

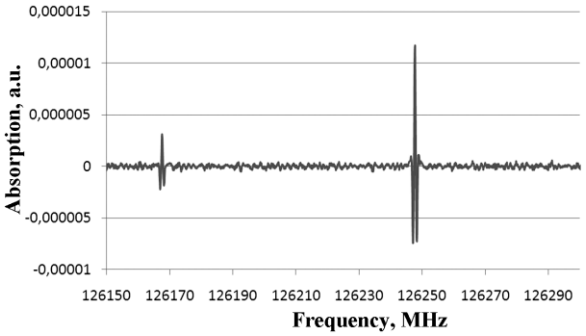

Fig. 4 The record of subTHz absorption spectrum of formamid in "odor" of summer wheat "Sitara"

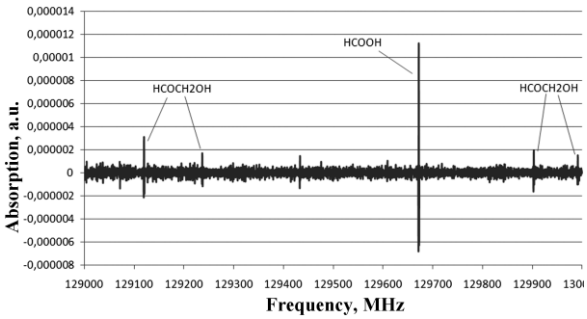

Fig. 5 The record of subTHz absorption spectrum of "odor" of winter wheat "Nemchinovskaya-17"

Fig. 3,4 shows the spectrum of formamide (NH2CHO) at 122.388 GHz 122.402 GHz, 126.168 GHz and 126.248 GHz [2,3], recorded when heated, when the grain sample begins to turn black, in the absorption spectra of the "odor" of "Sitara" wheat. The presence of formamide may be a consequence of the defeat of the grain by necrotrophic parasites. During evolution process, they developed a system of protection against toxic substances produced by the dying of infected cells, while one of the products of the transformation of toxic compounds is formamide.

The recording of the spectral region in the "odor" of winter wheat seeds of the variety "Nemchinovskaya-17" is shown in Fig. 5. A series of glycolaldehyde absorption lines (HCOCH2OH) at frequencies of 129120.22 MHz, 129.236 GHz, 129.902 GHz, 129.990 GHz [2,3] and formic acid (HCOOH) at the central frequency of 129.671 GHz have been detected. The appearance of glycolaldehyde, apparently, is characteristic of a multicomponent gas mixture that appears during the heat treatment of plants or the self-heating of grain during storage. Thus, the appearance of glycolaldehyde was detected by the pyrolysis of cellulose [4], which is one of the main components of the cell walls of plants. The appearance of formic acid in the gas mixture of a sample of wheat during heat treatment requires additional studies.

The applicability of the method of subTHz transient spectroscopy for studying of grain of various cereal crops for the diagnosis of their condition and the detection of fungal diseases was shown.

This work was carried out in the framework of state targets N 0035-2014-0206 and financially supported by the Russian Foundation for Basic Research (grant N 18-42-520050 r_a_povoljie, N 17-00-00184 KOMFI, N18-52-16017)

References

1. Vaks, V.L., Domracheva, E.G., Chernyaeva, M.B., Pripolzin, S.I., Revin, L.S., Tretyakov. I.V., Anfertev, V.A., Yablokov, A.A., Methods and approaches of high resolution spectroscopy for analytical applications //Opt Quant Electron (2017) 49: 239

2.Pickett H. M. Submillimeter, Millimeter, and Microwave Spectral Line Catalog. JPL Molecular Spectroscopy// H. M. Pickett, E. A. Cohen, B. J. Drouin, J. C. Pearson California Institute of Technology. http://spec.jpl.nasa.gov/ftp/pub/catalog/catform.html, 2003

3. C. P. Endres, S. Schlemmer, P. Schilke, J. Stutzki, and H. S. P. Müller, The Cologne Database for Molecular Spectroscopy, CDMS, in the Virtual Atomic and Molecular Data Centre, VAMDC//J. Mol. Spectrosc. 327, 95–104 (2016)

4. Cole, Daniel Paul, "High resolution mass spectrometry for molecular characterization of pyrolysis products and kinetics" (2015). Graduate Theses and Dissertations. 14342. http://lib.dr.iastate.edu/etd/14342

Definition of thresholds of the heating effects of THz radiation on cancer cells

A.A. Avseenko[1], M. K. Khodzitsky[2]

[1]ITMO University, Saint-Petersburg, Russia, arishkaavseenko@niuitmo.ru
[2]ITMO University, Saint-Petersburg, Russia

The main objective of the investigation is to determine the threshold parameters of THz radiation for its use in non-invasive therapy and diagnosis of cancer. This paper presents a model that allows identifying and calculating the thermal effects caused by THz radiation. The possibility of using these effects for the diagnosis and treatment of cancer is also being considered.

Cancer is a tumor formed by epithelial tissues that covers almost all human organs. Modern statistics show that every year cancer is registered in 10 million people around the world. In Russia, cancer mortality ranks second after heart and vascular diseases. (see [1]) Nowadays, medicine has achieved good success in the field of oncology, but the problem is that there is still no effective cure for cancer cells, and timely diagnosis in the early stages is a huge range of different tests. Therefore, it is important to create an effective technique aimed at diagnosing and combating cancer.

The scientific novelty of the study is determined by the fact that it examines the currently little-known thermal effects (see [2,3]) that occur when exposed to THz radiation (see [4]).

This model performs calculations (by solving the equation of thermal conductivity using the Debye model) for a cylindrical sample of water (see [5]), with the radiation frequency from 0 THz to 25 and temperatures from 0 C° up to 100 C°. The program interface includes several input parameters such as incident radiation parameters, sample parameters, coordinates and environmental conditions. The experimental values are presented in the table below:

Input parameter	Value
Radial coordinate	[-2:2]
Input power, mWt	1
Beam radius, mm	5
Initial temperature, K	295
Frequency, THz	1
Sample radius, mm	50
Sample thickness, mm	5

Figures 1 and 2 illustrate the results. It is obvious that with these values of the input parameters, the temperature increase reaches from 0.035 degrees in the center of the sample to 0.02 degrees at the periphery.

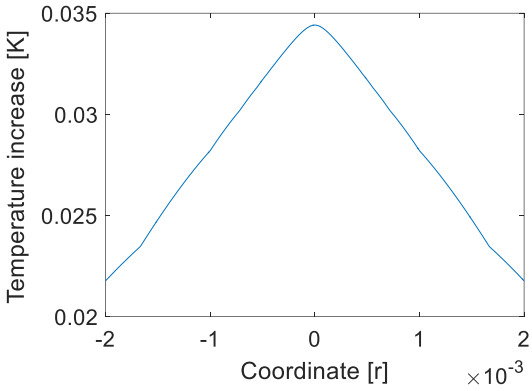

Fig. 1. The temperature increase in the sample along the radial coordinate

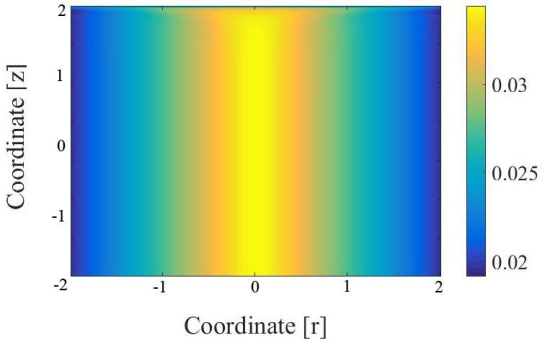

Fig. 2. The temperature increase in the sample caused by exposure to THz radiation

In addition, this model assumes the possibility of using the results of real experiments. Firstly, in the experiment, the cultivation of a line of cancer cells is carried out. Then their optical parameters are determined on the pulse THz spectrometer, such us the dispersion of the complex permittivity and the refractive index. The obtained parameters are loaded into the program. The results may lead to the conclusions about the value of the input parameters of radiation that can cause apoptosis of cancer cells and apply THz radiation for the diagnosis of diseases.

References

1. *Maksimova T. M., Belov V. B.* The morbidity and mortality of malignant neoplasms in Russia and some foreign countries // Problems of social hygiene, healthcare and history of medicine. 2012. No. 1. P.10.

2. *Borovkova, M., Serebriakova, M., Fedorov, V., Sedykh, E., Vaks, V., Lichutin, A., Salnikova, A., (...),*

Khodzitsky, M Investigation of terahertz radiation influence on rat glial cells // Biomedical Optics Express. 2017. Vol. 8. Issue 1. 2017. No. 276461. P. 273-280.
3. *Geyko, I.A., Smolyanskaya, O.A., Sulatsky, M.I., Parakhuda, S.E., Sedykh, E.A., Odlyanitskiy, E.L., Khodzitsky, M.K., Zabolotniy, A.G. Impact* of terahertz radiation on the epithelialization rate of scarified cornea // Progress in Biomedical Optics and Imaging - Proceedings of SPIE. 2015. Vol. 9542. No. 95420E.
4. *Borovkova, M., Khodzitsky, M., Demchenko, P., Cherkasova, O., Popov, A., Meglinski, I.* Terahertz time-domain spectroscopy for non-invasive assessment of water content in biological samples // Biomedical Optics Express. 2018. Vol. 9. Issue 5. No. 309306. P. 2266-2276.
5. *Torben T. L. Kristensen, Withawat Withayachumnankul, Peter Uhd Jepsen, and Derek Abbott*. Modeling terahertz heating effects on water // Optics Express. 2010. Vol. 18, No. 5. P. 4727-4739.

Study of blood and its components by terahertz pulsed spectroscopy

O.P.Cherkasova[1, 2], M. M. Nazarov[3], A. P. Shkurinov[4, 5]

[1]Institute of Laser Physics of SB RAS, Novosibirsk, Russia, o.p.cherkasova@gmail.com
[2]Tomsk State University, Tomsk, Russia
[3]Kurchatov Institute National Research Center, Moscow, Russia
[4]Crystallography and Photonics Federal Research Center, Russian Academy of Sciences, Moscow, Russia
[5]Lomonosov Moscow State University, Moscow, Russia

Introduction. The prospect of widely using THz radiation in medical diagnosis and therapy raises the question of interaction of human tissues with THz radiation. Blood is a fluid connective tissue. Blood consists of plasma, and cellular elements. There are three main types of cellular blood cells: red blood cells (RBC), white blood cells (leukocytes) and blood platelets (platelets). Blood plasma contains 90% of water, about 6.6 - 8.5% of proteins and other organic and mineral compounds, which are intermediate or final products of metabolism, transferred from some organs in others. Capillaries with blood are in the skin and can be exposed to THz radiation. Therefore it is important to know the dielectric properties of blood and its components in THz range. The report will provide a review of the known data and our own studies on THz time domain spectroscopy (THz-TDS) of blood and its components at normal states and some pathology.

Experimental. The study of blood and its components is performed both in transmission and reflection configurations. Blood is poured into a special cuvette with a thickness (d) of 50-500 μm. For d<100 μm thickness variation can introduce noticeable errors, especially in refraction index. In reflection spectroscopy, data variation is related to the time delay between the solution signal and the reference signal producing different slopes of the reflection spectrum phase. The results obtained by transmission spectroscopy are more reliable at lower frequencies (0.05–0.8 THz), whereas reflection spectroscopy is preferable for higher THz frequencies (1.0–2.5 THz) [1].

Results. THz absorption and reflection spectra of blood and its components have not any sharp spectral features (fig.1.) [1-3].

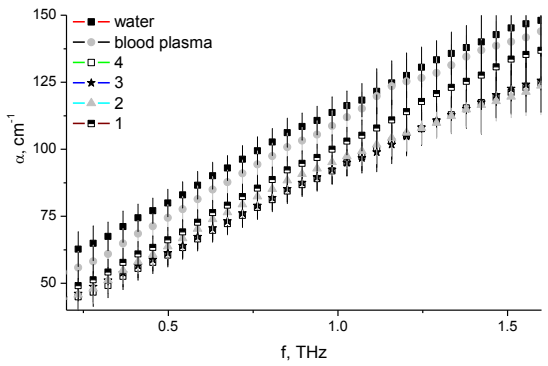

Fig. 1. Absorption coefficient of water, human blood plasma and RBC at different concentrations from $5.7 \cdot 10^6$ (1) to $7.32 \cdot 10^6$ (4) (cells/ml).

The shape of the spectra corresponds to the form of water spectrum, and for analysis, it is possible to use the two-component Debye model [1-3]. It was shown that there are some distinction in the Debye relaxation coefficients for the whole blood and its components [2]. A significant difference can observe in both the absorption and refractive index spectra of the whole blood and its thrombus: the coagulation and the formation of a thrombus have affected the absorption coefficient as well as the Debye coefficients [2, 4]. It was demonstrated the capability to distinguish thrombus formation at its early stage from uncoagulated blood by the change in the absorption coefficient at 200–270 GHz [4].

It has been shown that the absorption coefficient decrease linearly with increasing RBC concentration in whole blood [3, 5, 6]. The excellent linearity between the THz signal and the RBC concentration was also confirmed in a polyurethane resin tube using a THz imaging method. These results demonstrate that THz-TDS imaging can facilitate the quantitative analysis of blood [5].

It has been demonstrated that various biological substances of blood have a significant effect on its optical properties. A clinical study of ex-vivo fresh human whole blood showed that triglycerides and the number of RBC were two dominant factors to have significant negative correlation to the sub-THz absorption coefficients. This circumstance should be taken into account for future THz investigation in human whole blood [6]. The effect of blood glucose concentration on the optical properties of whole human blood was shown [7]. By investigating the THz spectra of different human blood, it was found out THz absorption coefficients reflect a high sensitivity to the glucose level in blood. With a quantitative analysis of 70 patients, it was demonstrated that the THz absorption coefficients and the blood glucose levels have a linear relationship [8].

The reduction of the absorption of blood plasma from mice with experimental oncology (Ehrlich carcinoma) relatively that of healthy mice have been shown in paper [9]. The authors concluded that such components of whole blood as blood red cells and platelets make the major contribution to the blood absorption in the THz range and the changes in the composition of other components cannot be reliably detected using the methods of THz spectroscopy.

It has been shown that the absorption coefficient and the refractive index of diabetic rat blood plasma are small compared to those of water and plasma of healthy rats [1, 10]. The diabetic rats have a higher

level of glucose in blood and low protein concentration in comparison with healthy rats [10]. Assuming that the observed spectral changes are due to changes in the state of water in blood plasma, we have selected one of the parameters of the Debye model, $\Delta\varepsilon_1/\tau_1$, leading to the spectral features observed in the experiment. This change in the response of bound water can be the reason of the observed changes at increasing glucose concentration in blood plasma. We have demonstrated that when the concentration of glucose in blood rises to 24 mM (in rats with diabetes), $\Delta\varepsilon_1/\tau_1$ ratio decreases in 1.2 times [1].

We carried out a detailed study of the influence of glucose and protein concentrations on THz response of water solutions at 0.05-3.2 THz [11-13]. Different sensitivity to protein concentration in three spectral subregions, around 0.1, 1 and 3 THz was shown, which can influence the quantitative analysis of blood components. We proposed a simple method for analyzing experimental data [1, 11-13]

Conclusions. Whole blood and its components were studied by the THz-TDS method by a number of authors**.** The change of composition caused by pathological processes in the organism can considerably affect the optical properties of blood components in the THz frequency range. This can be used to create new rapid diagnostic methods. The cause of the detected differences was discussed with respect to variation in the terahertz response of water.

Acknowledgements. This work has been supported by Russian Foundation for Basic Research (project № 17-00-00275 (17-00-00270)).

References

1. *Cherkasova, O.P., Nazarov, M. M., Angeluts, A.A., Shkurinov, A.P.* Analysis of blood plasma at terahertz frequencies // Optics and Spectroscopy. 2016. V. 120(1). P. 50-57.

2. *Reid, C.B., Reese, G, Gibson, A.P., Wallace, V.P.* Terahertz time domain spectroscopy of human blood // IEEE J. Biomed. Health Inform. 2013. V. 3, No. 4. P. 363–367.

3. *Angeluts, A.A., Balakin, A.V., Evdokimov, M.G. et. al.* Characteristic responses of biological and nanoscale systems in the terahertz frequency range // Quantum Electronics. 2014. V. 44, No. 7. P. 614 – 632.

4. *Sun, C. K., Chen, H. Y., Tseng, T.F. et. al.,* High Sensitivity of T-Ray for Thrombus Sensing // Scientific reports. 2018. V. 8:3948, DOI:10.1038/s41598-018-22060-y

5. *Jeong, K., Huh, Y.-M., Kim, S.-H., et.al.* Characterization of blood using terahertz waves // J. Biomed. Opt. 2013. V. 18 (10), 107008.

6. *Tseng T.-F., You, B, Gao H.-C., et. al.* Pilot clinical study to investigate the human whole blood spectrum characteristics in the sub-THz region // Opt. Express. 2015. V. 23, No 7. P. 9440–9451.

7. *Gusev,S.I., Demchenko,P.S., Cherkasova, O.P., Fedorov, V.I., Khodzitsky, M.K.,* Influence of glucose concentration on blood optical properties in THz frequency range // Chinese Optics. 2018. V. 11(2). P. 182-189.

8. *Chen, H., Chen, X., Ma, S. et al*. Quantify Glucose Level in Freshly Diabetic's Blood by Terahertz Time-Domain Spectroscopy // Journal of Infrared Millimeter and Terahertz Waves. 2018. V. 39. P. 399.

9. *Smolianskaya, O.A., Kravtsenyuk, O.V., Panchenko, A.V. et al*. Study of blood plasma optical properties in mice grafted with Ehrlich carcinoma in the frequency range 0.1 –1.0 THz // Quantum Electronics. 2017. V. 47, No. 11. P. 1031 – 1040.

10. *Cherkasova, O.P., Nazarov, M.M., Smirnova, I.N., Angeluts, A.A., Shkurinov, A.P.* Application of Time-Domain THz Spectroscopy for Studying Blood Plasma of Rats with Experimental Diabetes // Physics of Wave Phenomena. 2014. V. 22, No. 3. P. 185-188.

11. *Nazarov, M.M., Cherkasova, O.P., Shkurinov, A.P.* Study of the dielectric function of aqueous solutions of glucose and albumin by THz time-domain spectroscopy // Quantum Electronics. 2016. V. 46, No 6. P. 488 – 495.

12. *Nazarov, M.M., Cherkasova, O.P., Shkurinov, A.P.* Properties of aqueous solutions in THz frequency range // Journal of Physics: Conference Series. 2017. V. 793. Doi:10.1088/1742-6596/793/1/012005.

13. *Nazarov, M. M., Cherkasova, O. P., Shkurinov, A. P.* Comprehensive Study of Albumin Solutions in the Extended Terahertz Frequency Range // Journal of Infrared Millimeter and Terahertz Waves. 2018. V. 39 (9). P. 840-853.

Morphological analysis of microglia in early postischemic period in the mouse local cerebral ischemia

Glyavina M.M.[1,2], Loginov P.A.[1], Dudenkova V.V.[1,2], Shirokova O.M.[1], Reunov D.G.[1,2], Karpova A.O.[1,2], Prodanets N.N.[1], Korobkov N.A.[3], Zhuchenko M.A.[4], Mukhina I.V.[1,2]

[1]Privolzhsky Research Medical University, Nizhny Novgorod, Russian Federation, mariyannov@gmail.com
[2]Lobachevsky State University, Nizhny Novgorod, Russian Federation,
[3]Saint Petersburg State University, Saint Petersburg, Russian Federation,
[4]Pharmapark LLC, Moscow, Russian Federation.

Ischemic stroke is one of the most frequent causes of death and disability of patients. Microglia is a unique example of immunocompetent cell in central nervous system that is capable protecting the brain from ischemic injury. Microglia are constantly surveying their microenvironment. Under pathological conditions microglia rapidly change their morphology and adopt activation states in order adequately react to the activation-causing stimuli. However, now there is no understanding of the specific physiological role of each of the morphological microglia phenotypes [1, 3, 6].

At present, drugs mainly aimed at minimizing the consequences of a stroke are intensely developed. One of the new lines in the development of neuroprotection methods in a stroke is to use a β- common receptor subunit (β-cR) with EPOR as a therapeutic target. One of microglia membrane's receptors is common receptor subunit (β-cR), which in the presence of a ligand can form a dimeric complex with erythropoietin. Carbamylated darbopoietin (CdEPO) (PHARMAPARK LLC, Moscow) was used as an agonist for this receptor. When the receptor is connected to erythropoietin, this triggers two types of reactions, namely, a positive one, which activates the protective mechanisms of damaged neurons, and a negative one, which is caused by the increasing number of erythrocytes, resulting in reformation of a thrombus and a rise in blood pressure [2,4]. Therefore, Carbamylated darbopoietin (CdEPO) (Pharmapark LLC, Moscow) is able protect neurons from ischemic damage, ignoring hemopoiesis, which prevents the increase in hematocrit. Approximately 80% of the thrombotic or thromboembolic strokes occur in the middle cerebral artery. Thus, a model of transient occlusion of the middle cerebral artery (tOCMA) was used to study the stroke pathogenesis mechanism [5].

The somatosensory cortex and the hippocampus play an important role in learning and memory processes. Therefore, were investigated the morphological characteristics of microglia in these areas of brain.

Laser radiation is used to image the dynamic of changing microglia morphological phenotype. An objective of this work is to study the proportion of microglia phenotype and their morphological characteristic after of the middle cerebral artery occlusion (MCAO) and CdEPO treatment, because this is important for assessing the development of ischemic damage. The report presents the results of microglia phenotype distribution in the somatosensory cortex and hippocampus of the mouse brain in the early post-ischemic period in the MCAO model.

For this experiment, we use C57BL/6 mice. Surgery has been made using a binocular microscope and under isoflurane anesthesia. One-hour exposure was proceeded by a 7-0 microfilament from Doccol Corporation. The animal behavior was tested on the first day after the injection. Preservation of basic activity and memory was studied with Open Field LE800S test, Shuttle Box LE916 (PanLab/Harvard Apparatus), "novel object recognition" test. CdEPO was injected after intravenously in 1, 3, 6, 12, 24, 48 hours after model of transient occlusion of the middle cerebral artery (tMCAO) (one-hour exposure) at 50 mkg/kg dose. Behavior was studied on the 4-th postoperative day. Brain is fixed in 4% paraformaldehyde (PFA). Microglia was marked with primary Iba-1 antibodies (Rabbit polyclonal) and secondary antibody with fluorescent agant AlexaFluor 555. Visualization was carried out by a ZEISS LSM 880 laser scanning confocal fluorescents microscope with an 40x immersion objective and a yellow-green spectrum filter. Paraffin coronal sections of the brain (5 μm thick) were studied. The images were processed using ImageJ and Python 3 software.

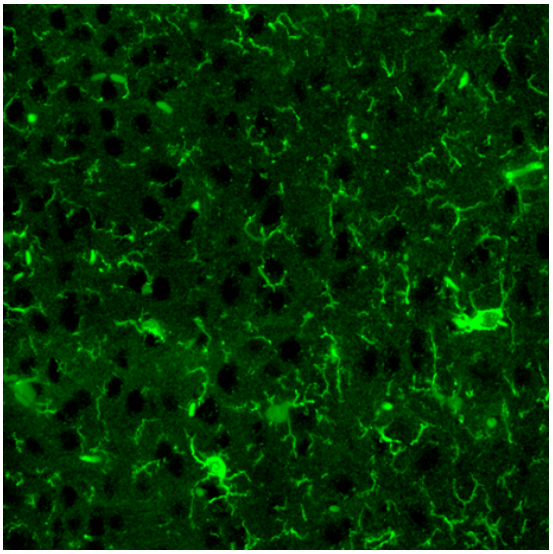

Fig. 1. Example of the processed image. The region of somatosensory cortex in the mouse brain (intact group). Green color corresponded to microglia (iba-1)

The morphological characteristics of microglia in the hippocampus is researched in the hemisphere with

an ischemic injury. The number of microglial cells in the hippocampus were decreased in control group. In the group with CdEPO injection, the number of microglia cells had not changed. The area of microglial cells decreased in the control group and rise in the group with injection of CdEPO on the 4th day after the MCAO in the hippocampus. On the 4th day after MCAO, there was a decline in the number of ramified microglia in the control group and in group with injection of CdEPO. However, generation of active microglia was rise in in the control group and in group with injection of CdEPO. Moreover, generation of amoeboid microglia was doubled in control group and had not changed in group with injection of CdEPO.

Microglia in the somatosensory cortex were studied in the hemisphere with an ischemic injury and in the contralateral zone. The number of microglial cells in the somatosensory cortex in the zone with ischemic damage decreased in control group. In the group with CdEPO injection there is an opposite situation: number of microglial cells approximated the intact values. The area of microglial cells decreased on the 4th day after the MCAO in the control group and in the group with injection of CdEPO. On the 4th day after MCAO, there was a decline in the number of ramified microglia in the control group as well as in generation of active and amoeboid microglia in both hemispheres. In the group with CdEPO injection, the number of resting microglia had not changed but the amount of activated microglia increased.

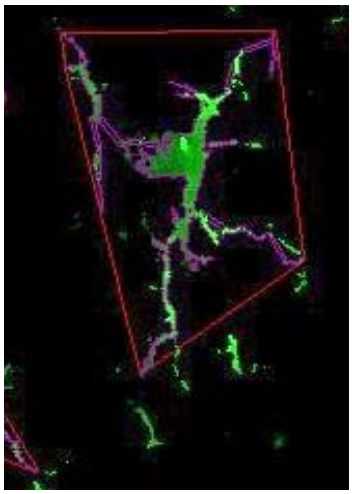

Fig. 2. Dendritic tree area (inside the solid - red in color online - line area). Area of contact microglia cell and microenvironment.

Change in microglia phenotypes and their morphology characteristic proportion in the group with CdEPO injection correlated with improved functional state of the animals after one-hour exposure: their motor activity restored, stress level was decreased and their memory was preserved.

The program of evaluating the morphological characteristics of microglia will help to understand the contribution of various microglia phenotypes to development of the ischemic damage and restoring the organism in the post-ischemic period. The ongoing research on regulation of microglia phenotypes proportion with CdEPO allows considering it as a promising neuroprotector giving a positive impact on the organism recovery in early post-ischemic period.

The reported study was funded by RFBR according to the research project № 18-34-00877

References

1. *Bachstetter AD et all*, Disease-related microglia heterogeneity in the hippocampus of Alzheimer's disease, dementia with Lewy bodies, and hippocampal sclerosis of aging// Acta Neuropathol Commun. , 2015 No. 23. P.3- 32.

2. *James M., Ian G. Young*, IL-3, IL-5, and GM-CSF signaling: crystal structure of the human beta-common receptor // Vitam Horm. 2006. No.74. P.1-30

3. *Karperien A. L et all.,* Box-counting analysis of microglia form in analysis of microglia form in schizophrenia, alzheimer's disease and affective disorder// Fractals, 2008. V. 16. No. 2. P. 103-107.

4. *Nataša Debeljak et all*, Erythropoietin and cancer: the unintended consequences of anemia correction // Front. Immunol., 2014. No. 5. P.563

5. *Rousselet1 E., Kriz J., Seidah N.G.,* Mouse Model of Intraluminal MCAO: Cerebral Infarct Evaluation by Cresyl Violet Staining // J. Vis. Exp., 2012. No.69. pii: 4038.

6. *Youngjeon Lee et all*, Therapeutically Targeting Neuroinflammation and Microglia after Acute Ischemic Stroke// BioMed Research International, 2014. Article ID 297241, P.1-9.

Investigation of interaction of THz radiation with blood components

S. I. Gusev[1], T. Zhang[1], V. Yu. Soboleva[1], Yu. A. Kononova[2], V. A. Guseva[1], P. S. Demchenko[1], E. A. Segykh[1], M. K. Khodzitsky[1]

[1]ITMO University, St. Petersburg, Russia, mail@gusev-spb.ru
[2]Federal Almazov North-West Medical Research Centre, St. Petersburg, Russia

Last decades THz radiation becomes more popular for spectroscopy and imaging tasks. One of the most important directions is biomedical diagnostics [1]. In comparing with visible, IR and microwave frequency ranges, THz radiation has more unexplored topics [2]. In context of wide spreading of diabetes mellitus disease, the blood glucose sensing in THz frequency range has especial importance.

This work represents list of our results, obtained step-by-step to develop non-invasive technique of blood glucose measurement. There is list of performed approaches described below: some show dependence between blood glucose concentration and optical properties, some experiments devoted to increasement of sensitivity to glucose and some to make measurement by non-invasive way.

All physical experiments had been performed with THz time-domain spectroscopy (TDS) in Terahertz Biomedicine lab of ITMO University.

First experiment objects were cotton clothes impregnated by fresh blood and measured in transmission way. [3] Each sample had been extracted from the same patient during short time period and had different glucose concentrations.

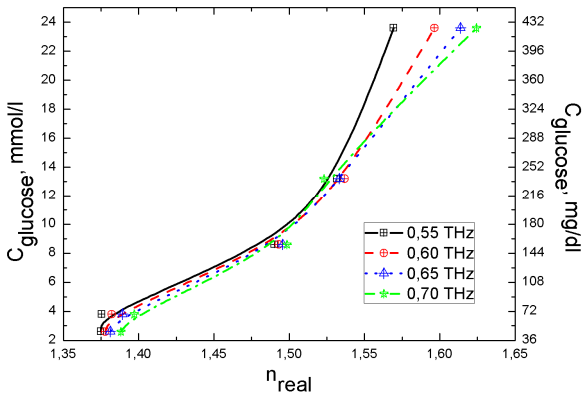

Fig. 1. Correlation between glucose concentration and refractive index had been observed at some frequencies

Second group of experiments was performed to reassure in results and increase accuracy. To prevent blood coagulation, water evaporation and provide stable thickness of the blood layer, special container had been produced. [4] It consisted from bottom and top parts, produced from polymethyl methacrylate. There were 2 experiments where blood layer was located inside the container. Blood samples had been from the same patient up to 8 times per experiment.

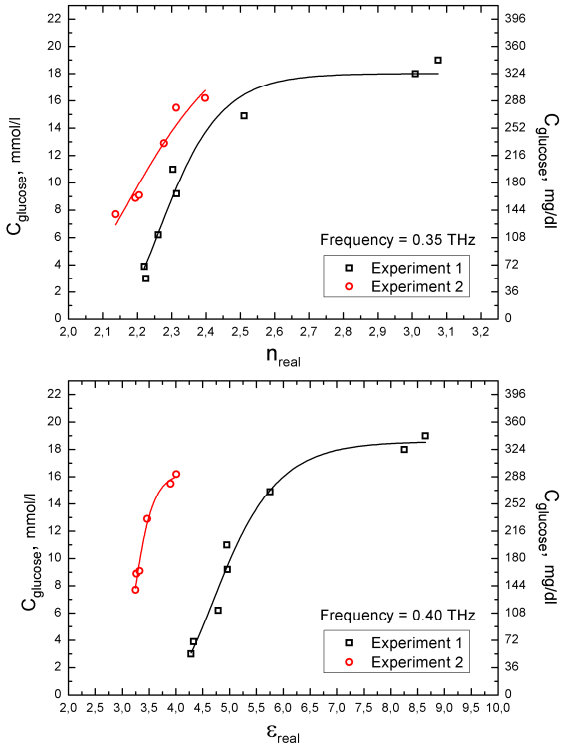

Fig. 2. Correlation behavior repeatability: for refractive index (top graph) as well as for permittivity (bottom graph)

Experimental results represented above showed method sensitivity to glucose level on condition of stable concentrations of other blood components (there were single patient during experiments). To estimate variability there were about 50 biosamples extracted from different patients, where concentration of components varies at each patient. [5] Each blood sample was analyzed for concentration of glucose, bilirubin, triglycerides, creatinine and uric acid by standard clinic laboratory tests. To observe influence of each component concentration on blood optical properties, observed parameters had been grouped by following principle: one parameter is varied, other are fixed.

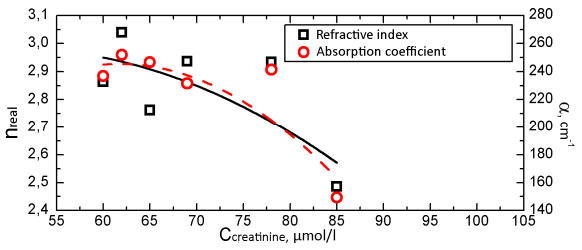

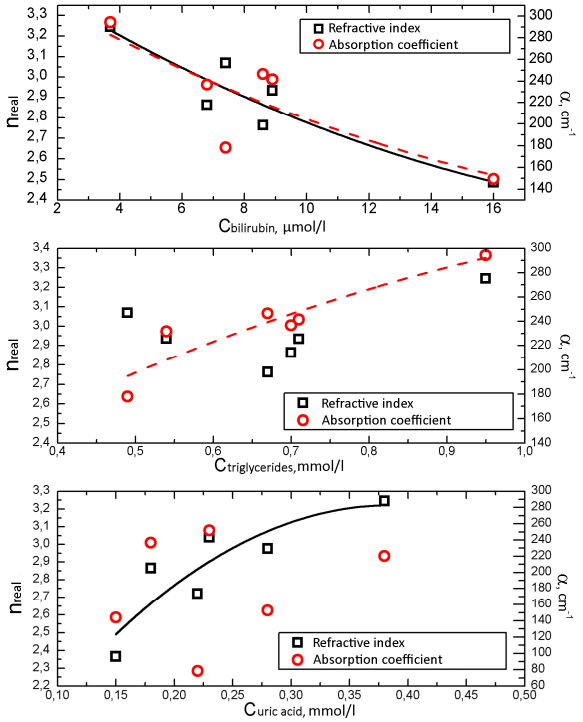

Fig. 3. In a number of cases there is possible to observe as blood optical properties in THz frequency range (such as refractive index and absorption coefficient) depend on concentrations of blood components.

To enhance sensitivity to glucose level there was performed simulation with band-pass aluminum metasurface with cross-shaped resonators sprayed on polyethylene terephthalate substrate. [6] Model consisted from this structure covered by thin layer of blood samples with the constant thickness. Each blood sample had different glucose concentration, their optical properties calculated before had been used during simuations.

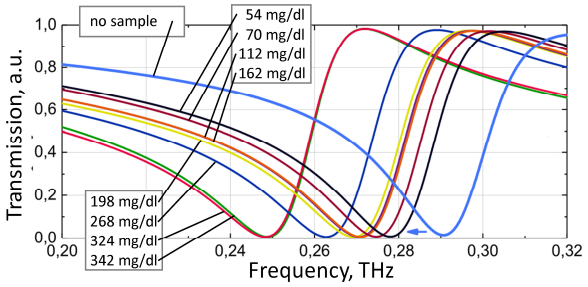

Fig. 4. With increasing of blood glucose concentration, we observe resonance frequency shift, which value directly correlates with blood glucose concentration.

For non-invasive technology development reasons, simulation of reflective experiment had been performed. [7] Described object consisted from nail plate and nail bed. Nail bed contains significant part of capillary filled by blood. Nail plate has stable thickness, flat surface and low absorption at THz frequencies. [8] As a result, modeled structure included listed objects, which were described by frequency dispersions of permittivity, calculated before with THz TDS in transmission mode.

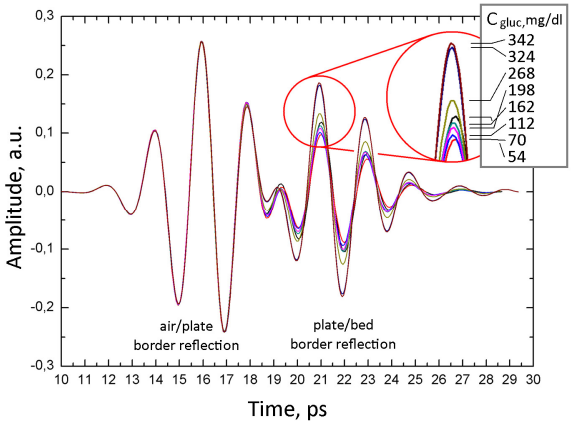

Fig. 5. Peak and peak-to-peak amplitude variations in reflection from plate/bed border shows tendency to correlation with blood glucose concentration.

Described series of studies shows dependence of blood glucose level and blood optical properties such as refractive index and permittivity. Influence of bilirubin, triglycerides, creatinine, uric acid concentration on whole blood optical properties had been investigated. There is metasurface-based method of increasing selectivity to glucose had been modeled and proposed. Non-invasive experiment using THz TDS had been simulated. Correlation of reflection amplitude and blood glucose had been observed.

There results showed THz radiation applicability and optimistic opportunities in the task of non-invasive glucose measurement.

References

1. *Pickwell, E., Wallace, V. P.* Biomedical applications of terahertz technology // Journal of Physics D: Applied Physics. 2006. V. 39, No. 17. P. R301.

2. *Tonouchi, M.* Cutting-edge terahertz technology // Nature photonics. 2007. V. 1, No. 2. P. 97.

3. *Gusev, S. I., et al.* Blood optical properties at various glucose level values in THz frequency range // Clinical and Biomedical Spectroscopy and Imaging IV. 2015. V. 9537. P. 95372A.

4. *Gusev, S. I., et. al.* Influence of Glucose Concentration on Blood Optical Properties in THz Frequency Range // Chinese Optics. 2018. V. 11, No. 2. P. 182–189.

5. *Zhang, T., et. al.* Qualitative analysis of blood components in terahertz frequency range // Scientific and Technical Journal of Information Technologies, Mechanics and Optics. 2018. V. 18, No. 5. (in Russian).

6. *Soboleva, V. Yu., Gusev, S. I., Khodzitsky, M. K.* Physical properties of macroscopically inhomogeneous media // Scientific and Technical Journal of Information Technologies, Mechanics and Optics. 2018. V. 18, No. 3. P. 377–383. (in Russian).

7. *Gusev, S. I., et al.* Study of glucose concentration influence on blood optical properties in THz frequency range // Nanosystems: Physics, Chemistry, Mathematics. 2018. V. 9, No. 3. P. 389–400

8. *Guseva, V. A., et al.* Optical properties of human nails in THz frequency range // Journal of Biomedical Photonics & Engineering. 2016. V. 2, No. 4.

Applications of THz laser spectroscopy and machine learning for medical diagnostics

Yu. V. Kistenev[1,2], A. V. Borisov[1,2], A.I.Knyazkova[1], E. A. Sandykova[1,2], V. V. Nikolaev[1], D. A. Vrazhnov[1]

[1]Tomsk State University, Tomsk, Russia, yuk@iao.ru
[2]Siberian State Medical University, Tomsk, Russia

THz spectroscopy allows to analyze molecular rotations associated with hydrogen bond breaking. But, the identification of pure compounds using molecular signatures with THz spectroscopy is still not straightforward because of the inherently broad spectral signatures in biotissue. A smooth shape THz of spectra causes a necessity to use the machine learning for tissue diagnosis using THz spectroscopy.

Typical machine learning pipeline includes the following steps (Fig.1) [1]:

- preprocessing of data;
- selection of informative features;
- development of predictive models for new data classification.

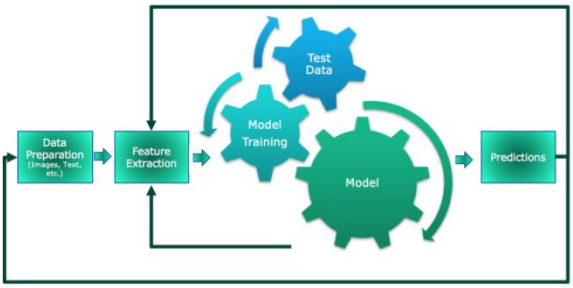

Fig.1. Typical machine learning pipeline.

In this report we present examples of peculiarities of machine learning applications for 2D THz image analysis. The results have been obtained using THz time-domain spectrometer (TDS) T-Spec by EXPLA in the range 0.2-3 THz.

At the preprocessing stage, in addition to filtering, various approaches to allocating areas of interest also should be considered. Automatic search of characteristic structures in the image is based on their formalized mathematical description of the image textures.

The example of preprocessing stage image transform connected with 2D THz TDS absorption spectra of formalin-fixed paraffin-embedded prostate cancer biopsy tissues is presented below. The goal is to remove artifacts of plastic substrate and paraffin from the image.

The Fig. 2 shows the spatial distribution of 2D THz image for a paraffin block without a sample and for a plastic substrate at frequencies 0.90 THz (Fig. 1a) and 1.05 THz (Fig. 1b).

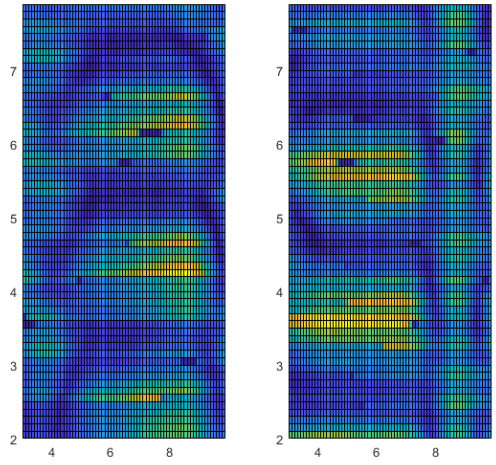

a

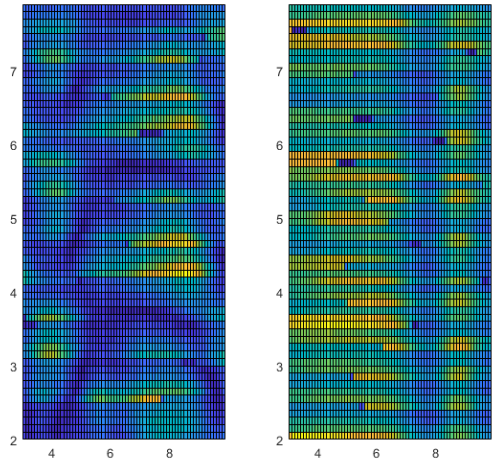

b

Fig. 2. Spatial distributions of the THz signal intensity for a paraffin block without a sample (on the left in each figure) and for a plastic substrate (on the right in each figure) at the frequencies: a - 0.90 THz and b - 1.05 THz.

The difference of absorption spectra allows to remove similar artifacts from the image. To realize it, an optimization algorithm was developed and implemented [3]. This algorithm allows to select pixels on the THz image with minimal influence of the paraffin and plastic substrates. The results of selection of a biopsy tissue on the 2D THz image are shown in the Fig.3.

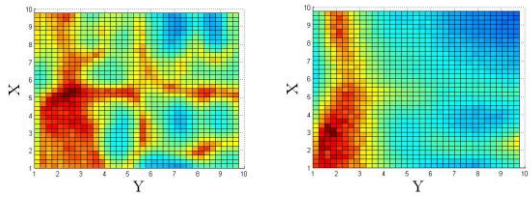

a b

Fig.3. Selection of a biopsy tissue on the 2D THz image: initial image (a), image after artifacts removing (b).

A key step in image analysis is the informative features selection, because the quality of the created predictive model is defined by the ability of spatial separation of the various groups under study in the feature space. One of the most effective method of this task solution is the principal component analysis (PCA). The basic idea of PCA is to find the reduced number of new variables, termed the principal components, which are enough for recovery of the initial variables, possibly with insignificant errors [2].

The PCA applications for 2D THz image analysis was done on animal model (rats) lymphedema tissue.

Lymphedema is a chronic progressive disease of the lymphatic system caused by abnormal accumulation of tissue fluid with a high protein content. Early diagnosis of this disease helps to choose the right treatment and prevent its further development. The existing methods of lymphedema diagnosing at early stages are not strict and consistent. The invention of THz microscopy opens up new possibilities for lymphedema tissue analysis in vivo.

Using the optimization algorithm, mentioned above, we carried out the classification of THz spectra of the most informative areas obtained in-vivo from the lymphedema affected leg tissue (result of surgery) and obtained from healthy leg tissue. The results show good enough the separation of lymphedema tissues from and healthy tissues in the space of the principal components (see Fig. 4).

The principal components are built using the THz spectra in the 0.8-1.0 THz spectral range. Note that the separation of the groups using THz imaging became possible after three weeks from the lymphedema surgery initiation.

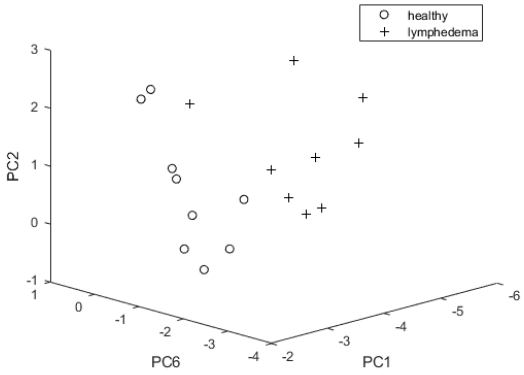

Fig. 4. Spatial distribution of the THZ spectra from lymphedema affected leg tissues and healthy leg tissues in the principal component space.

The work was carried out under partial financial support of the Russian Fund of Basic Research (grant No.17-00-00186, grant No. 18-42-703012 р_мол_а).

References

1. https://blog.westerndigital.com/machine-learning-pipeline-object-storage/machine-learning-pipeline/

2. L. Pomerantsev and O. Ye. Rodionova, Concept and role of extreme objects in PCA/SIMCA//*Journal of Chemometrics.* 2014. **28**(5), P.429-438.

3. Kistenev, Yu.V., Borisov, A.V., Knyazkova, A.I., Ilyasova, E.E., Sandykova, E.A., Gorbunov, A.K., Spirina, L.V. Possibilities of cytospectrophotometry of oncological prostate cancer tissue analysis in the TGz spectral range // Proc. of SPIE – XIII International Conference on Atomic and Molecular Pulsed Lasers (AMP17). - AMP100-94, 2018. No.10614-94.

The research method of a qualitative analysis of the composition of the blood in the terahertz frequency range

T. Zhang[1], Y.A. Kononova[1,2], M.K. Khodzitsky[1], P.S. Demchenko[1], S.I. Gusev[1], A.Y. Babenko[1,2], E.N. Grineva[1,2], Kublanova I.L.[1]

[1]ITMO University, Saint Petersburg, Russia

[2]Almazov National Medical Research Centre, Saint Petersburg, Russia

Introduction

The study of biochemical parameters of blood has an important role in the diagnosis of diseases, in honesty for patients diabetes mellitus. Of particular interest in this area is the study of the interaction of terahertz (THz) radiation with components of human blood. THz frequency range is remarkable in biomedicine in that it contains resonance frequencies of specific vibrational and rotational modes of biomolecules, therefore, using THz radiation, we can evaluate and determine the state of biological molecular bonds. In addition, THz radiation is very sensitive to different types of conformation of H_2O molecules with the rest of molecules contained in bio-samples. In the course of this work, the effect of bilirubin, triglyceride, uric acid, creatinine concentrations on the spectra of the refractive index and absorption of human blood in the THz frequency range was investigated, the results of which can be useful in the development of a method for analyzing blood composition.

Subject of study

The paper presents the study of blood biochemical composition (bilirubin, creatinine, triglycer-ides, uric acid) effect on its optical properties, i.e. refractive index and absorption coefficient, in terahertz fre-quency range was investigated.

Fig. 1. Measuring cell with a blood sample

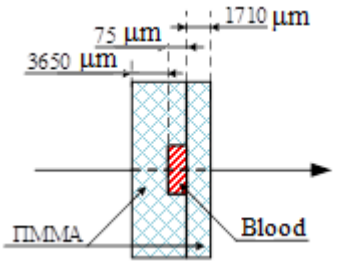

Fig. 2. Scheme of the measuring cell

Method

To obtain the values of the refractive index and the absorption coefficient, the method of terahertz time-domain spectroscopy was used in the transmission mode. Concentrations of total bilirubin, creatinine and triglycerides were measured in blood serum by the colorimetric method, the pseudokinetic method and the enzymatic method, respectively. The glucose level was determined in blood plasma by the enzyme method. All measurements of blood component concentrations were carried out at the Almazov National Medical Research Centre.

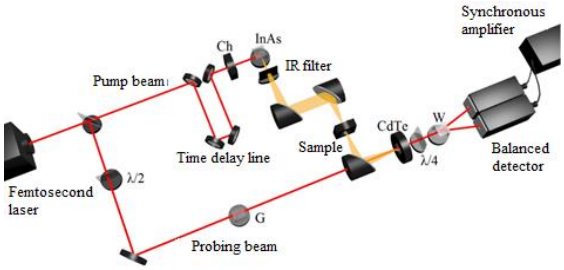

Fig. 3. Scheme of terahertz pulse spectrometer: λ/2 - half-wave plate; G - the Glan prism; Ch - breaker; λ/4 - the quarter-wave plate; W - the Wollaston prism

Main results

The optical properties of blood with various biochemical composition were ob-tained using terahertz time-domain spectroscopy at the

frequency of 0.4THz. It is shown that the refractive indices and the absorption coefficients of blood decrease with an increase in the concentration of bilirubin and creatinine. It has also been found that with an increase in the concentration of uric acid and triglycerides, the refractive index of blood increases and the absorption coefficient of blood decreases, respectively. The correlation between the refractive index and the concentration of triglycerides and the correlation between the blood absorption coefficient and the concentration of uric acid were not revealed.

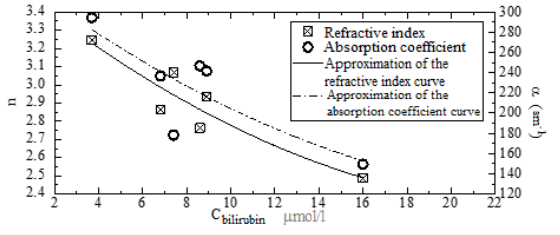

Fig. 4. Dependence of optical properties of blood on bilirubin concentration

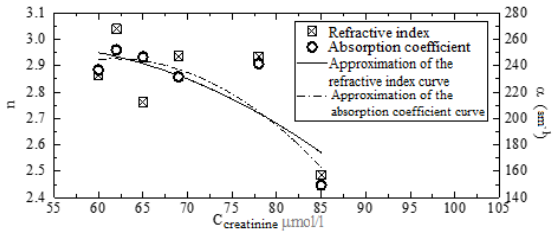

Fig. 5. Dependence of the optical properties of blood on the concentration of creatinine

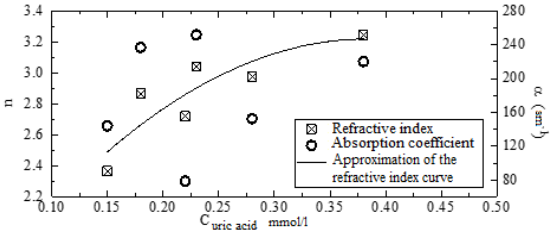

Fig. 6. Dependence of the optical properties of blood on uric acid

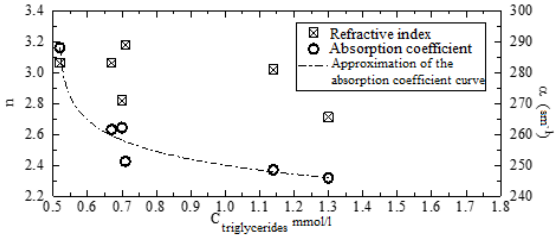

Fig. 7. Dependence of the optical properties of blood on the concentration of triglycerides

Practical significance

The observed correlations between the concentrations of blood components and the optical properties are useful in the development of a new technique for blood analysis.

References

1. Juvenile Diabetes Research Foundation Continuous Glucose Monitoring Study Group, Fox LA, Beck RW, Xing D. Variation of interstitial glucose measurements assessed by continuous glucose monitors in healthy, nondiabetic individuals // Diabetes Care. 2010. V. 33. N 6. P.1297–1299. doi: 10.2337/dc09-1971
2. Zhang X.C., Xu J. Introduction to THz wave photonics. Springer, 2010. 246 p.
3. Son J.H. Terahertz biomedical science and technology. CRC Press, 2014. 355 p.
4. Gusev S.I., Borovkova M.A., Strepitov M.A., Khodzitsky M.K. Blood optical properties at various glucose level values in THz frequency range // European Conference on Biomedical Optics. Munich, Germany, 2015. P. 95372A. doi: 10.1364/ECBO.2015.95372A
5. Gusev S.I., Demchenko P.S., Cherkasova O.P., Fedorov V.I., Khodzitsky M.K. Influence of glucose concentration on blood optical properties in THz frequency range // Chinese Optics. 2018. V. 11. N 2. P. 182–189. doi: 10.3788/CO.20181102.0182

Spectroscopy of solutions in the low frequency extended THz frequency range

Nazarov Maxim[1], O. P. Cherkasova[2, 3], A. P. Shkurinov[4, 5]

[1]Kurchatov Institute National Research Center, Moscow, Russia, nazarovmax@mail.ru
[2]Institute of Laser Physics of SB RAS, Novosibirsk, Russia
[3]Tomsk State University, Tomsk, Russia
[4]Crystallography and Photonics Federal Research Center, RAS, Moscow, Russia
[5]Department of Physics and International Laser Center, M.V.Lomonosov Moscow State University, Russia

One of the most important biological components of the living systems is water. It is the main informative feature and simultaneously the main obstacle for tissue and bio-solution spectroscopy in THz range. Its intensive absorption in this frequency range, on the one hand, limits its penetration into the samples, but, on the other hand, allows one to consider it as the subject of a separate fruitful study [1-4]. Water molecules form hydrogen bonds (HB) with their neighbors to construct the water network. Currently, water can be divided on bulk water (it does not form bonds with biomolecules) and hydration or bounded water (it surrounds biomolecules and interacts with them). Thus, in the solution, a considerable part of water molecules are in the form of a hydration shell – Fig 1.

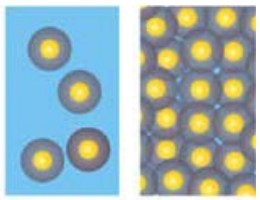

Fig. 1. Components of the solution: free water (blue background), bounded water (gray circles), solute molecules (yellow circles). Dilute solution (a) and saturated solution (b). After [4]

Bound or free water makes a valuable contribution to the THz response of biological objects. This allows us to use THz spectroscopy as a powerful tool to study different forms of water in a wide class of biological media, including the macromolecules in aqueous solutions. Actually, we do not measure the solute, its contribution is negligible. We measure how the solute modifies the solvent, the appearance and the structure of hydration shell around the solute molecules. To detect small changes in the solution smooth spectra, we should precisely describe solvent properties in a broad spectral range.

We describe a number of models of a water solution dielectric permittivity, which are applicable in the THz frequency range. We give a detailed description of biological solutions (protein and sugar solutions, blood components), analyze modern measuring techniques. All known processes (relaxation and dumped oscillation) in polar solutions below the tens of THz have very broadband responses, so it is essential to combine several experimental techniques, each for its own spectral range, to obtain spectra over many octaves. From the low frequency side, it is well established dielectric spectroscopy; from the high frequency side, it is FTIR and it is THz-time-domain spectroscopy (TDS) between them.

The main relaxation process (at 0.02 THz) reflects the cooperative reorientational dynamics of the dipole moment. It is assigned to the cooperative reorientation time of hydrogen-bonded bulk water molecules involving HB switching events. The oscillation processes indicates the overdamped modes, which correspond to several known vibration modes in the THz region: the bending mode between two water molecules forming the hydrogen-bond (at 1.5-2 THz); the intermolecular stretching of water is assigned to a hindered O...O translation (at 5.4 THz) *etc*.

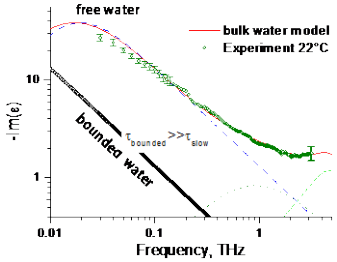

Fig. 2. Slow relaxation shift of bounded water spectra.

To fit dielectric function of water a well-known model with Debye-type relaxation and over-dumped oscillator components is usually applied [1-4].

$$\varepsilon(\omega,C)=\varepsilon_{\infty}+\frac{\Delta\varepsilon_1(C)}{1+i\omega\tau_1}+\frac{\Delta\varepsilon_2}{1+i\omega\tau_2}+\frac{A_1}{\omega_{01}^{\ 2}-\omega^2+i\gamma_{01}\omega}+... \qquad (1)$$

where τ_1 and τ_2 are relaxation times for the first (main) relaxation process and the second ('fast') relaxation term; $\Delta\varepsilon_i$ are the contributions into permittivity from corresponding relaxation; A_1 is amplitude; w_{01} is frequency; γ_{01} is the linewidth of the oscillator term. Slow relaxation spectra of bounded water are shifted to much lower frequencies – Fig.2, thus, in GHz and THz range bounded water has smaller absorption and dispersion. That is the main reason of solution spectra changes. In general, we should use the effective medium approximation for the total spectrum; in a more simplified case, we should take into account the volume fractions of the three solution components with different spectral responses.

The most widely-exploited method of solution measurements using THz spectroscopy implies studying the THz-wave transmission through a thin (50–100 μm) cuvette. In such measurements, even a small

uncertainty of the analyte layer thickness might cause a noticeable error in the reconstructed THz dielectric response. Thus thick cuvette is preferable. It gives considerable advantages in low frequency part of the THz spectra, where water transmission is not so small. For the high THz frequencies, the attenuated total reflection (ATR) measurement approach is preferable, since it does not suffer from strong water absorption and implies measurements of a bulk sample; thus, eliminating an error of layer thickness measurements. Actually, these methods have considerable overlap of the spectral operation range; thus, we combine the results obtained by transmission and reflection in order to achieve a broader spectral operation range and more reliable data for water solution spectroscopy [1].

Once the water spectrum is precisely measured and described, one can proceed to water solution analysis. The spectra of aqueous protein or saccharides solutions with not extremely high concentration are almost completely determined by the spectral properties of the solvent water. Therefore, there are reasons for application of Eq. (1) to describe permittivity of such biological media as aqueous solutions. To detect small-scale changes in solutions we have normalized the transmittance (and reflectance) of the solution T_{BSA} to that of water – Fig 3.

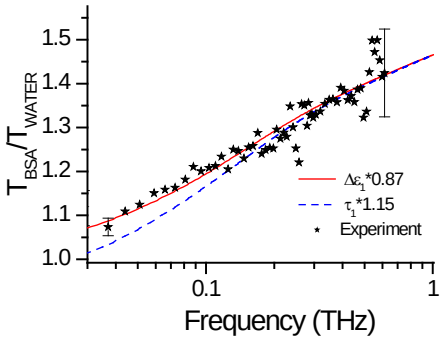

Fig 3. Transmission spectra of BSA 100 mg/ml water solution in a 500 μm cell, normalized to the case of water in the same cell, experimental data – open circles. Solid lines – model transmission with the same thickness and normalization. Red line with modified $\Delta\varepsilon_1$*0.87 ($\Delta\varepsilon_1/\tau_1$=0.87) and blue line with modified τ_1*1.15 ($\Delta\varepsilon_1/\tau_1$=0.87).

To identify the reasons for the THz transmission changes of BSA solutions we have compared the experimental spectra to the relative transmission of modified model of water [1]. Such a simplified approach, implying variation of a single parameter $\Delta\varepsilon_1(C)$, describes well the experimental spectra of aqueous solutions (particularly, of sugars and proteins) in the frequency range of at least 0.03 to 3.2 THz, which is important for practical applications of THz-TDS systems. Such a difference is best fitted by a decrease in the amplitude of the slow relaxation amplitude $\Delta\varepsilon_1$. An alternative approach is to use $\tau_1(C)$ as the only varied parameter instead of $\Delta\varepsilon_1$. At frequencies above f=0.3 THz, it is mathematically almost equal to vary τ_1 or $\Delta\varepsilon_1$ because $\omega\tau_1>>1$. In any case, in this THz band, 80 % of the spectral response is determined by the slow relaxation and its parameters, while contributions of the remaining processes in Eq. (1) are relatively small and weakly depend on the concentration.

Since there are practically no standards and calibrated instruments in the THz range, before studying a new system, it is necessary to achieve an agreement of the measured data with the well-known literature results on the THz dielectric response of some ”reference” solute, for example, glucose.

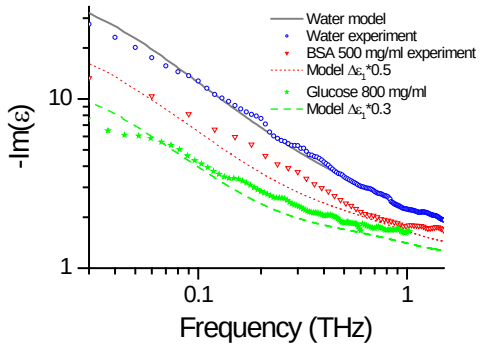

Fig 4. Dielectric function spectra of almost saturated solution of BSA (500 mg/ml) and of glucose (800 mg/ml) and of distilled water. Solid lines – model transmission with modified $\Delta\varepsilon_1$*0.5 for BSA and $\Delta\varepsilon_1$*0.3 for glucose. Symbols – experimental data.

Remarkable that different models lead to almost equal values of complex dielectric function in the frequency range where the models overlap.

Other important questions to be discussed in the talk are: Can we distinguish proteins from saccharides in water environment from the THz spectra shape? Are there narrow/resolvable spectral features of biomolecules in water environment below 5 THz? How can we extract the pure spectra of bounded water? What is useful in saturated solution spectra? When it is necessary to apply effective model for the solution?

Acknowledgements

The reported study was funded by RFBR project № 17-00-00275 (17-00-00270), 18-52-00040.

References

1. *Nazarov, M.M., Cherkasova, O.P., Shkurinov, A.P.* Study of the dielectric function of aqueous solutions of glucose and albumin by THz time-domain spectroscopy // Quantum Electronics. 2016. V. 46, No 6. P. 488 – 495.

2. *Shiraga, K., Adachi, A., Nakamura, M., Tajima, T., Ajito, K., Ogawa, Y.* Characterization of the hydrogen-bond network of water around sucrose and trehalose: Microwave and terahertz spectroscopic study // The Journal of Chemical Physics. 2017. V. 146 (10). P. 105102.

3. *Ellison, W. J.* Permittivity of pure water, at standard atmospheric pressure, over the frequency range 0–25 thz and the temperature range 0–100°C // Journal of Physical and Chemical Reference Data. 2007. V. 36 (1). P. 1–18.

4. *B. Born, B., Havenith, M.* Terahertz Dance of Proteins and Sugars with Water // J Infrared Milli Terahz Waves. 2009. V. 30. P. 1245–1254.

Application of THz radiation for *in situ* control of eye cornea hydration level

I.Ozheredov[1], M.Prokopchuk[1], T.Safonova[2], E.Sikach[2], P.Solyankin[3], A.Angeluts[1], A.Balakin[1,3] and A.Shkurinov[1,3]

[1]Lomonosov Moscow State University, Moscow, Russian Federation, ozheredov@physics.msu.ru
[2]Eye Diseases Institute, Moscow, Russian Federation
[3]Institute on Laser and Information Technologies of RAS, Branch of the FSRC
"Crystallography and Photonics" RAS, Shatura, Moscow Region, Russian Federation

The epithelium of the cornea and conjunctiva needs continuous moistening. With closed eyelids, the tear fluid fills the entire space, and when open, it spreads over the anterior surface of the eye forming a thin film. Tear film has a thickness of 4 - 7 μm and performs protective, metabolic and optical functions. The direct involvement of the corneal and conjunctival epithelium into formation of tear film was demonstrated in [1]. The tear film covers the whole corneal and conjunctival surface, from the area of transition from the keratinous multilayered epithelium of the eyelid skin edges to the non-corroborating multilayer epithelium of the conjunctiva and up to the corneal center. Thus it allows considering the tear film as one of the corneal layers.

Numerous causes leading to the loss of normal properties and structure of the tear film, lead to changes in the water-electrolyte balance. They also cause a decrease in the volume of tear fluid, a decrease in sensitivity and a development of corneal epitheliopathy. A complex of signs of the corneal and conjunctival epithelium lesion due to a decrease in the quality and/or amount of tear fluid defines a concept of 'dry eye syndrome' [2].

The assessment of pre-corneal tear film is a leading direction in the diagnosis of dry eye syndrome. In clinical practice the most common method for determining the stability of the tear film is Norn test. Non-invasive methods for studying the stability of a tear film include thioscopy. Confocal microscopy expands the possibilities of studying the anatomy of the cornea at the level of its microstructure. It has been shown recently [3,4] for *in vivo* measurements of corneal tissue hydration and tear film dynamic control the terahertz (THz) reflectometry might be efficiently used.

In the present study we apply frequency-domain THz reflectometry technique for sensing of the ocular surface system. Our study allows the dynamic control of pre-corneal tear film thinning and sensing of corneal tissue hydration level in clinical applications.

The concept of the proposed technique was based on THz photomixing approach. Typical photomixer consists of two independent tunable laser sources yielding the difference frequency in a desired THz region by heterodyning. Two laser beams with different frequencies light a photoconductive antenna (PCA), where running fringes with the THz difference frequency excite carries in the semiconductor material. The solid-state lasers are used as elements of a laser heterodyne. The single-mode selection of the laser is done using distributed feedback (DFB) - the diffraction grating technologically etched close to the p-n junction of the diode structure. PCA consists of an electrical dipole and semiconductor quick enough to produce carriers in time with the beat frequency. When the heterodyned laser beams light the surface of the semiconductor, than carriers appear in the material. If the metal antenna is polarized with some voltage then carriers give a periodical short circuit for the antenna and PCA converts the photocurrent into a THz wave.

The proposed apparatus was based on two DFB diode lasers with precise resonator temperature control. The lasers generated narrow 10 kHz line in the range of 1530 – 1608 nm with average power of 22 mW each. X-type fiber optical beam splitter with the splitting ratio 50/50 combined both lasers output. The outputs of the splitter were connected to the THz emitter and receiver - low-temperature InGaAs bow-tie PCA (BATOP GmbH). The bias voltage for the THz emitter (0/6 V, 40 kHz) was provided by the function generator. The difference frequency range of DFB lasers allowed tuning of the output THz radiation within a range of 0.04-0.1 THz. High-density polyethylene lens (HDPE) with focal distance of 30 mm focused THz signal to the ocular surface system. The specularly reflected THz signal was guided through second similar HDPE-lens into the receiver PCA module. The digital lock-in amplifier SR 810 (Stanford Research Systems) was used to measure the resulting photocurrent. Both THz emitter and receiver were were embeded into the clinical ophthalmic apparatus (Fig.1) allowed measuring the eye reflection in THz range simultaneously with using of the other standard ophthalmological methodic.

For the *in vivo* study the special experimental protocol was developed. For each human eye cornea the reflected signal versus time was measured and reflection coefficient was calculated. Each measurement started at the time of eye opening. During the measurement series the testee human was requested to keep the eye open as long as possible. The same time he was able to close the eye as soon as he willing doing that. The measurements continued until the next eye closing.

Fig. 1. THz reflectometer setup embedded into ophthalmic apparatus

The THz reflectivity of the cornea demonstrates the dehydration dynamics (Fig.2). Such dependency may be fitted by the special function and decreases with the time. At a time of eye closing the reflectivity decreases and remains constant while the eye is closed. After the next eye opening the reflectivity restores to the value similar one of the previous cycle. Based on the results of preliminary studies, it can be possible to measure of pre-corneal tear film dynamics.

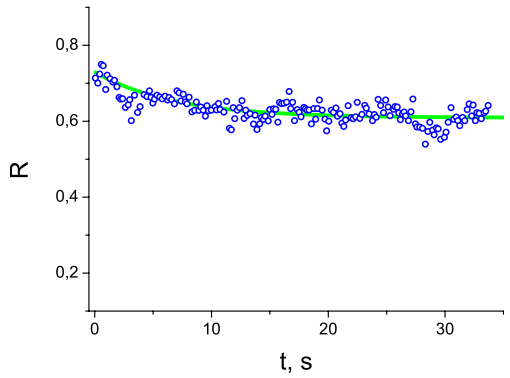

Fig. 2. Reflection coefficient of the ocular surface system as a function of time

Fig. 2 illustrates an example of the ocular surface system THz reflection coefficient versus time. This graph was obtained for the cornea of testee human without any claims. In case of complains on dryness in the eyes and suspicion of dry eye syndrome the dynamics of reflection coefficient change would be more changeable. Norn tests for each testee human were performed and the behavior of the reflection coefficient dynamics for these patients possesses good correlation with the Norn test results.

The value of THz reflection coefficient at the right edge of the graph in Fig. 2 corresponds to the case of critical thinning of the tear film and very close to the value of tear film break up case. This value could be taken for estimation the reflection coefficient of the corneal tissue and calculation of the hydration level of this tissue.

To confirm the detected correlations, similar studies were carried out for three groups of subjects. In the first group of 10 people, the eyes of people who did not express subjective complaints of discomfort in the eyes or excessive lacrimation were considered.

The second group represented a sample of people with instability of tear film established by Norn test and subjective complaints of dryness. The third group included eyes with hypersecretion of tear glands confirmed by Shirmer test. These groups of tested humans with eye abnormalities included 13 and 7 subjects respectively.

The results of these studies, presented in the form of a histogram in Fig. 3, show a correlation between the value of the linear function slope and the established diagnosis.

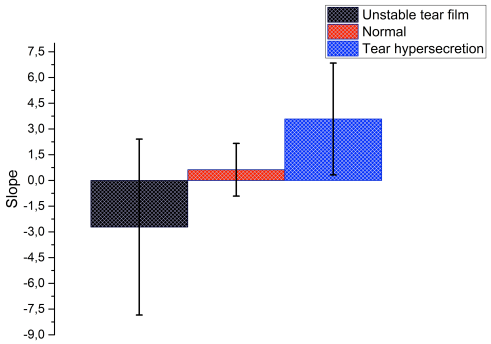

Fig. 3. Histogram of function slope coefficient for different eye type diseases

We showed the results of applications of the THz reflectometry to sensing of the ocular surface system and pre-corneal tear film. Our study allows the dynamic control of pre-corneal tear film thinning and sensing of corneal tissue hydration level in clinical applications *in vivo*.

This work was supported by RFBR (projects No.15-29-03900 and 17-00-00270).

References

1. *K.M.Meek*. The Cornea and Sclera. Boston, MA:Springer, 2008.
2. *V.V.Brzheskij, G.B.Egorova and E.A.Egorov*. Syndrome of ‘dry eyes’ and diseases of the eye surface: clinic, diagnosis and treatment. Moscow: GEOTAR-Media, 2016.
3. *Z.D.Taylor, J.Garritano, S.Sung, et al*. THz and mm-Wave Sensing of Corneal Tissue Water Content: In Vivo Sensing and Imaging Results. IEEE Transactions on Terahertz Science and Technology, vol.5, pp.184-196, 2015.
4. *I.Ozheredov, M.Prokopchuk, M.Mischenko, et al*. In vivo THz Sensing of Eye Cornea. Laser Physics Letters, vol.15, 055601, 2018.

A device to inspect a skin cancer tumour in the terahertz range, transferring the image into the infrared

A.V. Postnikov[1], K.A. Moldosanov[2], N.J. Kairyev[2], V.M. Lelevkin[2]

[1]University of Lorraine, Metz, France, andrei.postnikov@univ-lorraine.fr
[2]Kyrgyz-Russian Slavic University, Bishkek, Kyrgyzstan

The sensitivity of the THz radiation to water, which is one of the most important components of the biological tissue, can be used in practical schemes of visualizing a tumour. Namely, the water molecules absorb throughout the entire THz band (0.1–10 THz) [1], and the water content in cancerous tumours is higher than in normal tissues. One can think of a setup using the transmission geometry (see Fig. 1), which would normally involve *in vitro* study of a thin, clinically prepared tissue sample. In this approach, the necessary contrast for imaging the tumour and discerning it from the normal tissue is provided by enhanced water content in cancer cells. Otherwise, the fact that the THz waves cannot penetrate moist tissue motivated for the development of imaging in the reflection geometry, better suited for investigations *in vivo*, the most straightforwardly in relation with the skin cancer (Fig. 2). The reflectance of THz radiation, and hence the contrast in imaging the area with cancer cells, is enhanced as the water temperature in them increases [2,3,4,5]. To heat water in cancer cells, the gold nanoparticles (GNPs) can be premediately delivered therein; corresponding techniques are known [6,7]. Then the tumour is non-invasively treated by irradiating with near-infrared (NIR) laser beam at ~650–1350 nm wavelength (this is the so-called "therapeutic window" where light has its maximum depth of penetration into the tissues). Under irradiation, the surface plasmons are excited in the GNPs; on dumping out the plasmons, the water is heated around the nanoparticles in cancer cells. In consequence, the cancer cells start to reflect the incident THz radiation even more efficiently. The feasibility of the THz imaging of the body with skin cancer in reflection geometry have been demonstrated in [8].

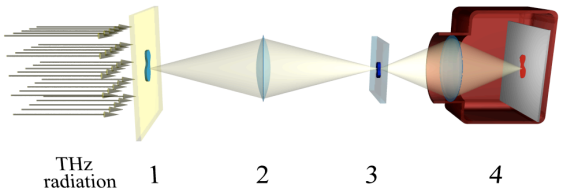

Fig. 1. Transmission mode for *in vitro* studies: 1 – a tissue sample, 2 – the THz objective (high resistivity float zone silicon, high density polyethylene or Teflon®), 3 – THz-to-IR-converter, 4 – highly sensitive IR camera

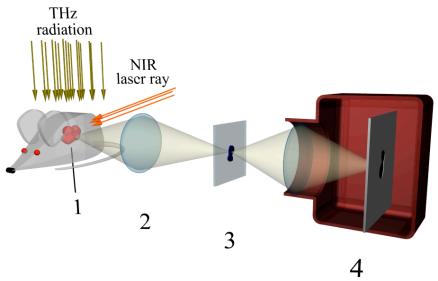

Fig. 2. Reflection mode for *in vivo* imaging with a usage of the near-infrared (NIR) laser for excitation of surface plasmons in GNPs inside a tumour (for heating water in cancer cells): 1 – tumour, 2, 3, 4 – the same as in Fig. 1

The nature of the THz radiation source to be used is not crucial for the present contribution; we note, nevertheless, that a possible design for such source was suggested in [9], having, as its working element, gold nanobars or nanorings which ought to be irradiated by microwaves in order to emit THz photons with energies within the full width at half maximum of the longitudinal acoustic phononic density of states of gold (16 –19 meV, i.e., 3.9 – 4.6 THz), with a maximum at about 4.2 THz (17.4 meV). In Ref. [10] it was shown that gold nanorhombicuboctahedra could be used as emitters of radiation at 0.54 and at 8.7 THz, important for the THz imaging of human skin cancer, in the context of findings of Ref. [11, 12] and possible impact on the improvement of spatial resolution.

The essential element for the hence suggested THz inspection device is the THz-to-infrared converter consisting of a layer (a matrix) of GNPs deposited onto (or, embedded into) a substrate, transparent in both THz and IR ranges. In both setups outlined by Figs. 1 and 2, the image (in the THz rays) originating from the tissue sample (position 1) is projected by the objective (position 2) onto the two-dimensional THz-to-IR-converter (position 3). The GNPs, on irradiation with THz rays, convert the energies of THz photons into heat, being so the bright spots for subsequent detection by a highly sensitive IR-camera (position 4). In this quality, commerciably available devices can be considered, which allow nowadays the temperature sensitivity of 14 to 50 mK [13,14].

A preliminary description of the scheme has been outlined by us in Ref. [15]. The present analysis reiterates the physical mechanism, which includes an excitation of the Fermi electron via an adsorption of a THz photon, and the subsequent relaxation with releasing a longitudinal phonon. The constraints imposed by size and shape of the nano-objects are discussed, along with the manifestation of the momentum and energy conservation laws in the preference for different channels of relaxation. Technically, calculations are done of the THz irradiation power needed to be delivered in order to enable detection of a thermal image developed on the converter by IR cameras. The static distribution of temperature around a

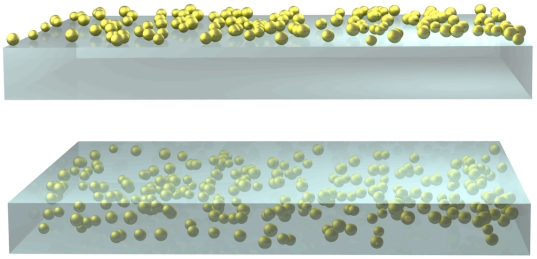

Fig. 3. Schemes of the THz-to-IR converter: above – in the form of a substrate transparent in THz wavelength range with GNPs; below – in the form of a matrix transparent in THz wavelength range with embedded GNPs

GNPs of different sizes embedded in a substrate (specifically, Teflon® and silicon have been considered) was calculated, along with dynamical onset of the temperature, in order to estimate the size and reaction time of bright spots being created in the converter, and thus to judge about the latter's spatial resolution and reaction time.

Concerning the realization of the THz-to-IR converter, two schemes shown in Fig. 3 may come into discussion. That in the form of a thick film with embedded GNPs (Fig. 3, lower scheme) seems preferable over single-layer deposition (Fig. 3, upper scheme), because it allows to achieve larger "projected" density of GNPs per surface unit, avoiding at the same time to place them too closely.

The obtained theoretical results demonstrate that the suggested approach can be realized with the THz-to-IR converter made of Teflon® film of ~ 0.1 nm thickness, containing GNPs of ~10 nm diameter. With this, the suggested design is only waiting for practical tests.

Considering a possible impact in medicine, one can recall that, in contrast to X-rays, the THz radiation is not ionizing and not harmful to living organisms. The development of practical THz imaging setups is one of the "hottest" areas in nanotechnology-supported modalities for the cancer diagnostics. The THz diagnostics in reflection geometry allows for non-invasive *(in vivo)* THz imaging of skin cancer's surface features. It could be performed *in situ*, without time losses on standard *in vitro* histological tests. Other areas of dermatology, where the THz imaging in reflection geometry might be advantageous, are (*i*) skin burns and wound inspection through bandages, and (*ii*) monitoring the treatment of skin conditions (like psoriasis), since this allows to avoid the direct contact with the skin as *e.g.* under ultrasound investigation. Even if the THz radiation is strongly absorbed by water and does not penetrate tissue to any significant depth, the use of the transmission geometry and clinically prepared tissue samples (both of inner organs and the skin) may offer an interesting extension to established techniques. One can mention in this relation that the THz imaging is less costly than, for instance, the magnetic resonance study.

References

1. *Berry, E., Walker, G. C., Fitzgerald, A.J., Zinov'ev, N.N., Chamberlain, M., Smye, S. W., Miles, R.E., Smith, M.A.* Do *in vivo* terahertz imaging systems comply with safety guidelines? // J. Laser Appl., 2003. V. 15, No. 3, P. 192–198.

2. *Rønne, C., Thrane, L., Åstrand, P.O., Wallqvist, A., Mikkelsen, K.V., Keiding, S.R.* Investigation of the temperature dependence of dielectric relaxation in liquid water by THz reflection spectroscopy and molecular dynamics simulation. // J. Chem. Phys., 1997, V. 107, No. 14, P.5319–5331.

3. *Son, J.H.* Terahertz electromagnetic interactions with biological matter and their applications. // J. Appl. Phys., 2009, V. 105, No. 10, P. 102033-1–102033-10.

4. Oh, S.J., Maeng, I., Shin, H.J., Lee, J.,.Kang, J., Haam, S., Huh, Y.M.,.suckSuh, J., HiukSon, J. Nanoparticle contrast agents for terahertz medical imaging. // 33rd International Conference on Infrared, Millimeter and Terahertz Waves (IRMMW-THz 2008, Pasadena, USA). P. 1–2. DOI: 10.1109/ICIMW.2008.4665813.

5. *Oh, S.J., Kang J., Maeng, I., Suh, J.S.,. Huh, Y.M., Haam, S., Son, J.H.* Nanoparticle-enabled terahertz imaging for cancer diagnosis. // Opt. Express, 2009, V. 17, No. 5, P. 3469–3475.

6. *Loo, C., Lowery, A., Halas, N., West, J., Drezek, R.* Immunotargeted nanoshells for integrated cancer imaging and therapy. // Nano Lett., 2005. V. 5, No. 4, P. 709–711.

7. *El-Sayed, I.H., Huang, X., El-Sayed, M.A.* Selective laser photo-thermal therapy of epithelial carcinoma using anti-EGFR antibody conjugated gold nanoparticles. // Cancer Lett., 2006. V. 239, No. 1, P. 129–135.

8. *Woodward, R.M., Cole, B.E., Wallace, V.P., Pye, R.J., Arnone, D.D., Linfield, E.H., Pepper, M.* Terahertz pulse imaging in reflection geometry of skin tissue using time-domain analysis techniques. // Physics in Medicine and Biology, 2002, V. 47, No. 21, P. 3853-3863.

9. *Moldosanov, K.,. Postnikov, A.* A terahertz-vibration to terahertz-radiation converter based on gold nanoobjects: a feasibility study. // Beilstein J. Nanotechnol., 2016, V. 7, P. 983–989.

10. *Postnikov, A.V., Moldosanov, K.A.* Suggested design of gold-nanoobjects-based terahertz radiation source for biomedical research. // Nanotechnology, 2018. V. 29, No. 28, P. 285704 (8 pp).

11. *Wallace, V.P., Fitzgerald, A.J., Pickwell, E., Pye, R.J., Taday, P.F., Flanagan, N., Ha, T.* Terahertz pulsed spectroscopy of human basal cell carcinoma. // Appl. Spectrosc. 2006, **60**(10), 1127–1133

12. *Pickwell, E., Wallace, V.P.* Biomedical applications of terahertz technology. // J. Phys. D: Appl. Phys., 2006, V. 39, No. 17, P. R301– R310.

13. Infrared Cameras Inc., Mirage 640 P-series | fixed / process control calibrated thermal camera with temperature measurement. https://infraredcameras.com/thermal-infrared-products/mirage-640-p-series/.

14. FLIR A6700sc MWIR, science-grade MWIR INSB camera. https://www.flir.com/ products/a6700sc-mwir/.

15. *Moldosanov, K.A., Postnikov, A.V., Lelevkin, V.M,. Kairyev, N.J.* Terahertz imaging technique for cancer diagnostics using frequency conversion by gold nano-objects. // Ferroelectrics, 2017, V. 509, P.158–166.

THz absorption spectra of glucose and its polymers

Anna Semenova[1], Yu.S. Guseva[1,2] V.L. Vaks[1,2], A.N. Panin[1], D.A. Babarina[2], S.S. Morunova[3], A.S. Vilkov[3]

[1]Institute for Physics of Microstructures, Nizhny Novgorod, Russia, semenanna@yahoo.com
[2]Lobachevsky State University, Nizhny Novgorod, Russia,
[3]Nizhny Novgorod State Agricultural Academy, Nizhny Novgorod, Russia

Introduction

Terahertz (THz) spectroscopy has tremendous potential for biological and medical applications. First, THz spectroscopy is used for chemical analysis of multicomponent gas mixture, particularly, for exhaled breath (EB) analysis. There are narrow absorption lines in the THz range caused by quantum transitions between rotation levels of molecules in gas phase and different lines are corresponded with different chemical substances. Because the exhaled breath is a mixture of not only oxygen, nitrogen and carbon dioxide but more than 800 gases which concentrations reflect the level of homeostasis, as well as the severity of pathological conditions, EB analysis is a perspective method for diagnostic purposes. It is non-invasive and unpainful for patients. The probability of infection transmission is very low for the method because there is no contact with any biological fluids. It is rather inexpensive and very sensitive for small concentration of measured substances. Therefore, THz spectroscopy of exhaled breath is becoming a powerful method of medical diagnostics, especially, incipient stage diagnostics and prevention of socially important diseases [1, 2].

Second, THz technic could provide a powerful tool for investigating and even manipulating of biomolecules *in situ*, in water solution, and *in vivo*, in cell cultures and whole organisms. THz irradiation is no ionizing and is treated as non invasive for biomolecules [2, 3] if irradiation power and exposure times do not exceed some threshold. Worth noting that absorption of organic samples and liquid water in the THz frequency range is caused by low-frequency vibration modes of the molecules, which occur than large groups of atoms of the molecule move coherent, and hydrogen bond net oscillation in the sample. Hydrogen bonds stabilize spatial structure of biomolecules whereas which determine eigen frequencies of the molecular vibration modes. Therefore, THz spectra are unique for each spatial structure of each molecule [2 - 6]. Worth noting that biomolecular spatial structures commonly described in the terms of configuration and conformation are crucial for their functions. Configuration means the mutual bracing of chemical bonds in a molecule, it can not change without chemical reaction. For example, R and S forms of any chiral molecule differs as left and right hand corresponds to different conformations. It is well known that even R and S isomers of rather simple molecules such as amino acids represent different pharmacological effects [7]. Conformation means momental spatial displacement of atoms in a molecule, it continuously oscillating near some equilibrium state by thermal fluctuations without any chemical reactions. Conformational state and dynamics determine biomolecular activity. For example, specificity of enzyme catalysis is caused by matching of space structure and electric charge displacement between the enzyme and substrate molecules; structural changes occurring at denaturation lead to loss of catalytic activity (notable that denaturation could be accompanied by no chemical conversion) [7, wiki 8]. Some conformational transitions are lethally dangerous, for example, PrP protein abnormal forms, so-called prions, stop execute their common functions and begin catalyze only PrP molecules conformational transmission from normal to the same abnomal form causing neurodegenerative diseases [прионы, 9]. Therefore there is necessary medicine task developing conformational diagnostics of biomolecules *in situ*, for example in water solutions, and *in vivo*, for example, in yeast cells for understanding how exactly they manage to control their specific prions [elements 10]. However, commonly used at present methods such as X-ray analysis, electronic and atomic force microscopy requires molecular crystals or adsorbed molecules. On the one hand, THz spectroscopy is becoming the urgent method investigating of conformational state and dynamics of biomolecules in liquid media that minimizes the influence on the explored molecules [2 - 6] On the other hand, there are announcements about non-thermal influence of strong THz field on cell life activity, cellular differentiation and animals behaviour [4, 5]. The reported effects manifested frequency dependance so powerful and frequency stable THz sources could be used for exciting specific conformational transitions, for example, for conversion from prion to normal form of PrP protein [11, 12].

Purposes

While THz spectroscopy shows great perspectives for diagnostics of molecular spatial structure,

nevertheless its practical application is obstructed by some problems mainly caused by rather short story of THz technic and, consequently, rather small experience in the field. There are not enough models pointing at what to look at in THz absorption spectra. Our work is aimed at comparative analysis of absorption spectra measured for water solutions of different carbohydrates with different concentrations. The explored samples include water solutions of monosaccharides glucose and fructose, disaccharide sucrose and polysaccharide amylose.

First investigation of dependance absorption spectra on concentration is planned for the glucose solutions with concentration varying from 10% to 40%. There is some possibility of deviation from the most common linear dependance because THz absorption of water-water and water-glucose hydrogen bonds differs and dependance of the amount of both types of bonds on the solution concentration is not linear at high concentrations.

Second investigation of molecular configuration influence on absorption spectra is planned for two isomers, glucose and fructose, prepared in form of water solutions with the same concentration.

Third there is planned absorption spectra comparison for water solutions of glucose and its polymer amylose for finding out any specific corresponds to structure of long linear molecule.

Final there is planned to compare the spectrum of solution containing 20% glucose and 20% fructose with the spectrum of 40% sucrose solution. A molecule of fructose could be hydrolyzed into two molecules (one glucose and one fructose) but in neutral solutions at room temperature both glucose-fructose mixture and sucrose are stable. Thus difference between the two spectra could be caused by difference between molecular structures with resembling chemical composition.

Experimental setup

The principal scheme of the experimental setup is shown on fig. 1, where S means source of monochromatic THz irradiation with frequency turnable in the range from 112,5 to 114,8 GHz, D means detector of THz irradiation and C means cell with liquid sample or pure water (control).

The distance between the cell and the detector was fixed while the distance between the cell and the source was variated. The detected power depends quasi periodically on the distance due to standing wave forming. There are two measurements for the each frequency and each sample with two different distances between the source and the cell corresponded to two neighbour maximums of detected power.

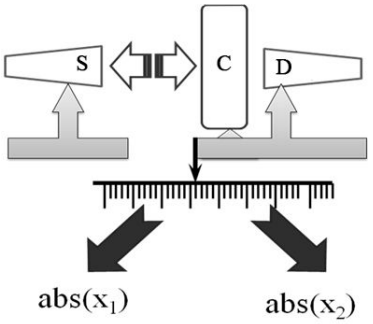

Fig. 1. Principal scheme of experimental setup. Two measurements were carried out for each sample and frequency.

Acknowledgements

The reported study was funded by RFBR according to the research project № 18-32-00328.

This work was carried out in the framework of state targets N 0035-2014-0206.

References

1. *Vaks, V.L., Domracheva, E.G., Sobakinskaya, E.A., Chernyaeva, M.B.* Exhaled breath analysis: physical methods, instruments, and medical diagnostics // Phys.-Usp. 2014. V. 57, No. 7. P. 684–701.

2. *Vaks, V.L., Domracheva, E.G., Sobakinskaya, E.A., Chernyaeva, M.B.* Methods and Instruments of High-Resolution Transient THz Spectroscopy for Diagnostics of Socially Important Diseases // Phys. Wave Phen. 2014. V. 22, No. 3. P. 177–184.

3. *Zhang, X.-C.* Terahertz wave imaging: horizons and hurdles // Phys. Med. Biol. 2002. V. 47. P. 3667–3677.

4. *Alexandrov, B.S., Phipps, M.L., Alexandrov, L.B., Booshehri, L.G. et. al.* Specificity and Heterogeneity of Terahertz Radiation Effect on Gene Expression in Mouse Mesenchymal Stem Cells // s. rep. 2013. V. 1184, No. 3. P. 1–8.

5. *Alexandrov, B.S., Gelev, V., Bishop, A.R., Ushevaet, A., et al.* DNA Breathing Dynamics in the Presence of a Terahertz Field // Phys. Lett. A 2010. V. 374, No. 10. P.1214–1217.

6. *Markelz, A., Whitmire, S., Hillebrecht, J. Birge, R.* THz time domain spectroscopy of biomolecular conformational modes // Phys. Med. Biol. - 2002 - 47; URL: stacks.iop.org/PMB/47/3797V. 57, No. 7. P. 684–701.

7. *Vol'kshtejn, M.V.* Biofizika // Nauka, Moscow 1988

8. *Koshland, D.E.* Application of a Theory of Enzyme Specificity to Protein Synthesis // Proc. Natl. Acad. Sci. U.S.A. 1958. V.44, No.2. P.98-104.

9. *Zuev, V.A.* Priony – osobyj klass vozbuditelej medlennyh infekcij cheloveka i zhivotnyh // RMZh 2013. V. 30. P. 1559–1566.

10. *Vaks, V.L., Domracheva, E.G., Sobakinskaya, E.A., Chernyaeva, M.B.* Exhaled breath analysis: physical methods, instruments, and medical diagnostics // Phys.-Usp. 2014. V. 57, No. 7. P. 684–701.

1. *Vaks, V.L., Domracheva, E.G., Sobakinskaya, E.A., Chernyaeva, M.B.* Exhaled breath analysis: physical methods, instruments, and medical diagnostics // Phys.-Usp. 2014. V. 57, No. 7. P. 684–701.

Hastings, D. E., Wang, J. K. The radiation impedance of electrodynamic tether with end connectors // Geophys. Res. Lett. 1987. V. 14, No. 6. P. 519–522.

2. *Bergman, D. J., Stroud, D.* Physical properties of macroscopically inhomogeneous media // *Solid State Physics: Advances in Research and Applications*, edited by H. Ehrenreich and D. Turnbull. New York: Academic Press. 1992. V. 46. P. 147–269.

Interaction of terahertz radiation with tissue phantoms: numerical and experimental studies

O. A. Smolyanskaya[1], Q. Cassar[2], M. S. Kulya[1], N. V. Petrov[1], K. I. Zaytsev[3,4], A. I. Lepeshkin[1], J.-P. Guillet[2], P. Mounaix[2], V. V. Tuchin[1,5,6]

[1] ITMO University, Saint-Petersburg, Russia, smolyanskaya@corp.ifmo.ru
[2] Bordeaux University, IMS Laboratory, Bordeaux, France
[3]Bauman Moscow State Technical University, Moscow, Russia
[4]Prokhorov General Physics Institute of the RAS, Moscow, Russia
[5]Saratov State University, Saratov, Russia
[6]Institute of Precision Mechanics and Control of the RAS, Saratov, Russia

Introduction

New biomedical devices require test objects to check their performance and periodic calibration to monitor the system efficiency over the time. A phantom is a bio-like object mimicking the intrinsic real-tissue properties that serves as a test object. A variety of phantoms are commercially available. Phantoms are already used in spectroscopy within various spectral range. However, currently, the THz frequency range suffers from a lack of investigations in this direction. Only the first steps have been performed [1]. In the present work, we investigate interaction of submillimeter radiation with the breast-mimicking and skin-mimicking phantoms. Results for breast-mimicking phantom were compared with numerical models based on a double-Debye model of the dielectric permittivity for different content of fat, fibrous and cancerous tissue. The wave front propagation using the angular spectrum representation was used to simulate the theoretical response of skin-mimicking phantoms.

Model of wavefront propagation

Electromagnetic fields can be represented in various ways. The angular spectrum representation is a numerical technique describing optical fields in a homogeneous media [2]. Optical fields are described as a superposition of plane waves and evanescent waves. A useful approach to describe optical field diffraction is to conduct the Fourier analysis at a given plane so that the different Fourier components of the field distribution are identified as plane waves propagating away from that plane in different directions. Thus taking less computation time for numerical reconstruction. This technique is preferable for the analysis of light diffraction by histological slides [3]. Angular spectrum representation consists of the following stages: (i) the representation of the field through the angular spectrum of 2D waves (Eq.1); (ii) multiplication by the transfer function that contains a complex refractive index of the object (Eq.2); (iii) the back transition from plane waves to the wave field in the calculated z-plane (Eq.3).

$$C\left(f_x, f_y, \nu\right) = \int_{-\infty}^{\infty}\int_{-\infty}^{\infty} G\left(x, y, \nu\right)_{z=0} \exp\left(-2\pi i\left(xf_x + yf_y\right)\right) dxdy \quad (1)$$

$$g_{x,y}\left(f_x, f_y, \nu, z\right) = C\left(f_x, f_y, \nu\right)\exp\left(-i\frac{2\pi\nu n(\nu)}{c}\sqrt{1-\left(\frac{f_x \cdot c}{\nu n(\nu)}\right)^2 - \left(\frac{f_y \cdot c}{\nu n(\nu)}\right)^2}\cdot z\right) \quad (2)$$

$$G\left(x, y, \nu, z\right) = \int_{-\infty}^{\infty}\int_{-\infty}^{\infty} g_{x,y,z}\left(f_x, f_y, \nu, z\right)\exp\left(2\pi i\left(xf_x + yf_y\right)\right) df_x df_y, \quad (3)$$

where $n(x, y, \nu) = n_{re}(x, y, \nu) + i \cdot n_{im}(x, y, \nu)$ is the spatial and frequency distribution of the complex index of refraction.

Materials and methods

a. Sample preparation

We have used three-component phantoms made of fat, protein and water of different content. Vegetable oil (10 – 75%), soya (13 – 75%) and water (0 – 70%) were homogenized to generate an emulsion. Then, the phantoms were deposited into vacuum packages.

b. THz-Spectrometer

The commercially available TPS 4000 (Teraview Ltd, UK) spectrometer working in reflection mode was used. The spectral range of the system is from 0.06 to 4.50 THz. The entire system was under an air-dried dome to limit the interaction of water molecules with generated pulses. Samples were mounted on a sapphire substrate during measurement. The sapphire cut was chosen not to exhibit a birefringence that would disrupt results of measurements [4]. Each sample was measured 5 times, independently, *i.e.* the sample was removed and replaced again into system.

c. Numerical modelling

A double-Debye model of the dielectric permittivity was used to compare optical properties of the three-component phantoms and some biological tissue (adipose, fibrous and cancerous) taken from our previous paper [5].

Results and discussion

The propagation dynamics of the pulsed THz radiation through a skin sample was numerically simulated in the temporal and spectral domains. The index of refraction,

n_{re}, absorption coefficient, α, as well as real, ε_{re}, and imaginary, ε_{im}, part of dielectric permittivity was calculated from the experimentally obtained data. Figure 1a depicts the time-domain spatial evolution of the THz pulse. Agreement between measured and simulated THz waveforms is confirmed by the comparison shown in Figure 1b.

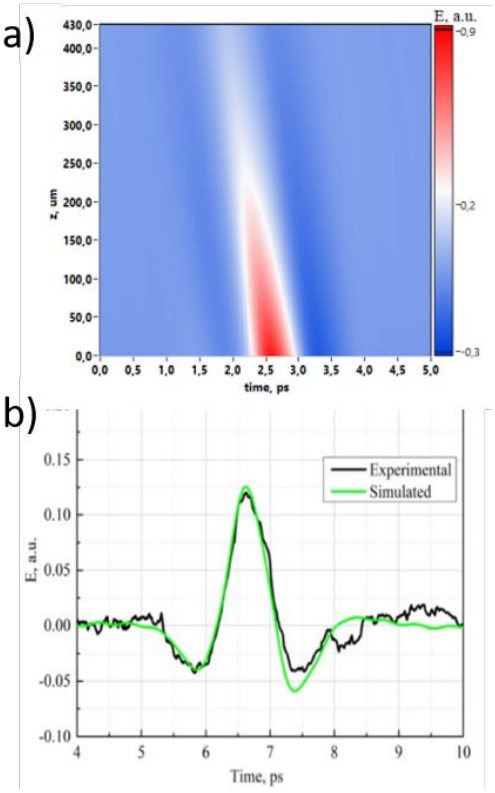

Fig. 1. Experimental and numerically simulated THz pulses propagated through a skin-mimicking sample. (a) THz spatial distribution. (b) THz waveforms.

In Figure 2 the spectral dependences of the absorption coefficient of the three-component phantoms consisting of fat, protein and water are depicted. It is shown that within the spectral window, the absorption coefficient of phantoms containing water exceeds the absorption coefficient of phantoms free of water. This is due to the fact, that water molecules, which strongly absorb THz radiations, are replaced by low absorbing components (fat and protein). Our results were compared with simulated signals of adipose, fibrous and cancerous tissues. taken from our previous paper [5].

Conclusion

To overcome the lack of knowledge on tissue-mimicking phantoms within the submillimeter spectral range, we conducted preliminary studies on skin- and breast tissue-mimicking samples. Simulations performed for skin-mimicking phantoms

have match the experimental spectral data. Thus demonstrating advantages of the technique used in this

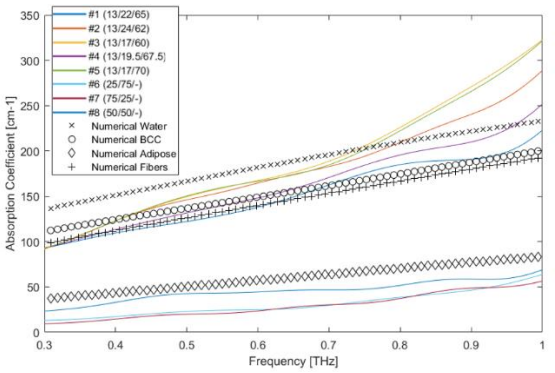

Fig. 2. Spectral dependences of the absorption coefficient of the three-component phantoms consisting of fat, protein and water in the THz frequency range (solid-colored lines) versus simulated signal of water and purely adipose, fibrous and cancerous tissue types.

study. The absorption coefficient spectral dependences extracted from measurements for breast-mimicking phantom, are clearly differentiated into two distinct groups. One for phantoms containing water and those being water-free. Such a discrimination is also shown via the double-Debye model of the dielectric permittivity. Thus, finding of a proper composition of tissue phantom is possible by an appropriate matching of model and experimental data. Deeper investigations are however still required to fulfill a set of phantoms that could be used to perform tissue measurement within the THz-range. Such a set would be profitable to design new medical THz-devices without human biopsy.

Acknowledgments

The reported study was funded by RFBR and CNRS according to the research project №18-51-16002, and by the Government of the Russian Federation (Grant 08-08).

References

1. *E Liakhov, O Smolyanskaya, A Popov, E Odlyanitskiy, N Balbekin, M Khodzitsky,* Fabrication and characterization of biotissue-mimicking phantoms in the THz frequency range // Journal of Physics: Conference Series. 2016. No. 735. P. 012080.

2. *Petrov, N. V., Kulya, M. S., Tsypkin, A. N., Bespalov, V. G., & Gorodetsky, A.* Application of terahertz pulse time-domain holography for phase imaging // IEEE Transactions on Terahertz Science and Technology, 2016, V. 6, No. 3, P. 464-472.

3. *O. A. Smolyanskaya, I. J. Schelkanova, M. S. Kulya, E. L. Odlyanitskiy, I. S. Goryachev, A. N. Tcypkin, Ya V. Grachev, Ya G. Toropova, and V. V. Tuchin* // Glycerol dehydration of native and diabetic animal tissues studied by THz-TDS and NMR methods // Biomedical Optics Express, 2018, V. 9, No. 3, P. 1198-1215.

4. *Q. Cassar, A. Al-Ibadi, Ia. Mavarani, Ph. Hillger, J. Grzyb, G. Macgrogan, Th. Zimmer, U.R. Pfeiffer, J.-P. Guillet, P. Mounaix* Pilot study of freshly excised breast tissue response in the 300 – 600 GHz range // Biomed Opt Express. 2018. V. 9 No. 7. P. 2930–2942.

5. *A. J. Fitzgerald, E. Pickwell-MacPherson, and V. P. Wallace,* Use of finite difference time domain simulations and Debye theory for modelling the terahertz reflection response of normal and tumour breast tissue // Plos One **9**, 1-9 (2014).

The influence of terahertz radiation on biochemical metabolism of blood in the experiment

A.G. Soloveva, P.V. Peretyagin, A.G. Polyakova, N.V. Didenko

Federal State Budgetary Educational Institution of Higher Education «Privolzhsky Research Medical University» of the Ministry of Health of the Russian Federation, Nizhny Novgorod, Russia, sannag5@mail.ru

In recent years, close attention has been paid to studies related to the impact of electromagnetic radiation (EMR) terahertz (THz) range on the living organism. Until now, the final idea of the ways and physical and chemical mechanisms of EMR THz action has not been formed, so it is important to identify all possible "points of application" of such an impact on biological systems [1]. Because the level of lipid peroxides reflecting the integrity of biological membranes changes under the action of different EMR ranges [2], and the antioxidant system controls the intensity of free radical processes, providing protection of cells and tissues [3], these systems were chosen to detect changes caused by THz radiation.

The aim of the work was to study the effect of electromagnetic radiation of the terahertz range on the functional and metabolic parameters of rat blood in the process of reparative regeneration.

Materials and methods

The experiment was carried out on 15 male Wistar rats weighing 250-300 g. in accordance with the requirements of the Geneva Convention "International Guiding Principles for Biomedical Research Involving Animals" (Geneva, 1990). The impact of EMR was carried out in the direct sound irradiation EMR THz (110-170GHz) from the experimental emitter apparatus "AMFIT" (N.Novgorod).

Animals were divided into 3 equal groups: 1– intact healthy rats, 2 – control – operated animals without any effects, 3 – operated animals with irradiation EMR THz at a dose of 0.12 MJ within the next 7 days (10 minutes 1 time per day). The impact was carried out on the base area of the displaced flap, coinciding with the localization of the skin projection of the center of vegetative regulation. Surgical intervention in 2 and 3 groups of rats and withdrawal from the experiment on day 7 after the operation was carried out under intramuscular anesthesia (Zoletil + Xyla).

Blood stabilized with sodium citrate (1:9) was used for the studies. Glucose and lactate concentrations were measured on a Super GL ambulance device (Germany) in plasma and red blood cells. The activity of lactate dehydrogenase (LDH) in direct (LDHdir) and reverse (LDHrev) reactions was determined on the spectrophotometer Power Wave XS (Bio-Tek, USA). The total content of nitric oxide metabolites was determined by the method of L.C.Green with coauthors in the modification of V. A. Metelskaya and N. G. Gumanova [4].

The intensity of lipid peroxidation (LPO) of a biological object by the level of malonic dialdehyde (MDA) in plasma and hemolysate of washed erythrocytes (1:10) [5], the activity of superoxide dismutase (SOD) [6] in hemolysate of washed erythrocytes (1:10) and catalase [7] in erythrocytes were determined by spectrophotometry.

The state of microcirculation and the degree of microcirculatory insufficiency with the analysis of the parameter of microcirculation (PM) characterizing the degree of tissue perfusion by blood, using wavelet analysis, were evaluated according to laser Doppler fluorometry on the analyzer of capillary blood flow LAKK-M (Russia).

Statistical processing was carried out using the program Statistica, version 6.0, using the Student criteria. Differences were considered statistically significant at $p<0.05$.

Results

In animals of group 2 the activation of LPO in erythrocytes was detected, MDA concentration increased by 20% compared to intact animals (Fig.1). In the erythrocytes of control animals compared with the intact group a compensatory increase of catalase specific activity on 17% (p=0.02) was registered, but a SOD activity decreased on 16% (p=0.003) (Fig.2). It indicated about an insufficient degree of compensation of the LPO by the antioxidant system in the operated animals.

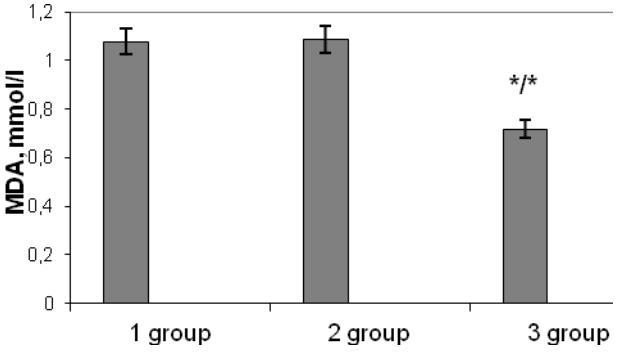

Fig.1. The concentration of malonic dialdehyde in the blood plasma of healthy and operated animals under the influence of EMR THz.
Note: * - differences are statistically significant compared to group 1; ** - differences are statistically significant compared to group 2.

The decrease of the intensity of LPO in plasma under the influence of THz-irradiation was observed. MDA concentrations in plasma decreased by 34% (relative to both comparison groups) under the influence of EMR THz.

The activity of enzymes of bioradical protection increased in the experimental group after irradiation of EMR THz. The most positive dynamics was observed for the SOD. SOD activity after surgery in the experimental group of animals increased by 30%

(p=0.018) compared to the control and reached the indicator of healthy animals. The activity of catalase also increased by 12% (p=0,025) compared to the rate of intact rats under the influence of irradiation. It reduces the free radical forms of oxygen and inactivates LPO. Consequently, THz exposure in the noise mode of radiation has an antioxidant effect through the activation of SOD and catalase, which, in turn, inhibit the release of catecholamines from the nerve endings and adrenal glands, as well as the action of these monoamines at the postsynaptic level [8]. Therefore, it is possible that one of the mechanisms that provide a decrease in the intensity of LPO under the action of EMR THz is the suppression of hyperactivity of one of the most important stress-implementing systems of the sympathoadrenal system.

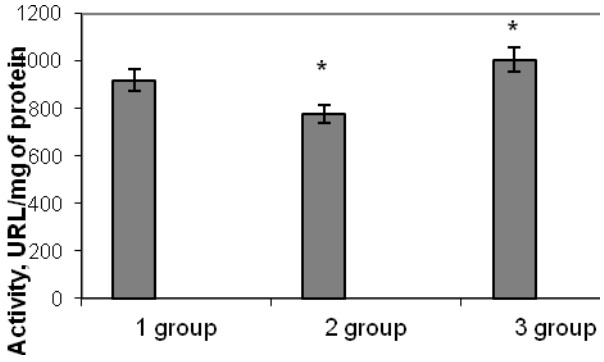

Fig.2. Activity of blood superoxide dismutase in healthy and operated animals under the influence of EMR THz

Note: * - differences are statistically significant compared to group 1; ** - differences are statistically significant compared to group 2.

Thus, in the experimental group of animals the predominance of antioxidant activity over the processes of lipoperoxidation was observed. It may indicates the inhibition of the biological oxidation system due to the suppression of reactive oxygen species under the influence of EMR THz. In response to the irradiation of the projection of the center of vegetative regulation, apparently, there is a neurohumoral activation of the antioxidant system, which blocks the processes of LPO. The revealed change in the direction of LPO processes under irradiation may be due to changes in the structure (conformation) of the cell surface of membrane components due to the weakening of hydrophobic bonds [1].

There was an increase in glucose and lactate in rats of the control group in plasma and erythrocytes. An increase in glucose concentration can contribute to a significant formation of free radicals through glycation reactions and autooxidation of glucose. The decrease of LDHdir on 33% in trauma in comparison with healthy animals.

EMR irradiation of THz in the noise range 110-170 GHz contributed to a decrease in the concentration of lactate in plasma and erythrocytes by 34% and 51%, respectively, compared with the animals of the control group. It was shown that under the influence of EMR THz activity of LDHdir increased on 47%, LDHrev – on 23% compared to the LDH activity of the rats without irradiation. In addition, it is possible that electromagnetic radiation promotes the use of lactate in carbohydrate metabolism in the formation of 2,3-diphosphoglycerate, the main source of energy in the body.

The zone of irreversible vascular changes in the flap at animals of 3 group after irradiation of EMR with a wide frequency range (110-170 GHz) containing spectra of the main metabolite molecules, was less pronounced in comparison with the control.

Since the most common among all microcirculatory disorders are local vascular spasm and decrease in blood flow rate, the registered preliminary data on animals confirm the spasmolytic mechanism of action of electromagnetic radiation of the THz range on the smooth muscle vascular wall of animals. At the same time, an increase in the content of nitrites and nitrates in the blood serum was revealed after irradiation of EMR THz.

Conclusion

The results showed that EMR of THz with a noise range of 110-170 GHz in ischemia led to an increase in the antioxidant status of the blood, as well as inhibition of peroxide states. It was shown that EMR THz of noise range 110-170 GHz increased the energy metabolism of blood in case the tissue ischemia.

References

1. *Bajinyan, S.A., Meliksetyan, A.M., Malakyan, M.G. et al.* // Millimeter waves in biology and medicine 2003. V.32, No 4. P. 12.

2. *Gapeev, A.B., Cheremis, N.K.* Mechanisms of biological action of electromagnetic radiation of extremely high frequencies at the cellular level // Biomedical technologies and Radioelectronics. 2007. No. 2-4. P. 44-61.

3. *Ulashchik, V.S.* Electromagnetic waves of the terahertz range and their therapeutic and prophylactic use // Questions of balneology, physiotherapy and physical therapy. 2007. No. 4. P. 3–7.

4. *Metel'skaya, V.A., Gumanova, N.G.* Screening method for determining the level of nitric oxide metabolites // Clinical laboratory diagnostics. 2005. No. 6. P. 15–18.

5. *Uchiyama, M., Mihara, M.* Analyt. Bbiochem. 1978. No. 86. P. 271.

6. *Sirota, T.V.* A new approach in the study of the process of adrenaline auto-oxidation and its use for measuring the activity of superoxide dismutase // Questions of medical chemistry. 1999. V. 45, No. 3. P. 109-116.

7. *Sibgatullina, G.V., Haertdinova, L.R., Gumerova, E.A. et al.* Methods for determining the redox status of cultivated plant cells: teaching aid. Kazan, Kazan (Volga) Federal University, 2011.

8. *Chuyan, E.N., Ravaeva, M.Y., Nikolskaya, V. A. et al.* Scientific notes of Taurida national University. V.I. Vernadsky. Series biology, chemistry. 2013. V. 65, No. 26. P. 223.

High resolution terahertz spectroscopy for medical, biological and agricultural applications

V. L. Vaks[1,2], E. G. Domracheva[1], S. I. Pripolzin[1], M. B. Chernyaeva[1]

[1]Institute for Physics of Microstructures RAS, Nizhny Novgorod, Russia, elena@ipmras.ru
[2]Lobachevsky University, Nizhny Novgorod, Russia

High resolution terahertz spectroscopy [1] is promising method for analysis of multicomponent gas mixtures including biological ones. Among the spectroscopic methods, the only approach to date that ensures a near-theoretical-limit sensitivity along with a good spectral resolution limited just by the Doppler effect is the nonstationary spectroscopy based on free dumping polarization effect. Other advantages of the spectrometers include easy-to-use configuration and measurement time of several microseconds that provide registration of unstable gases. Application of this method will also benefits in registration of gas-markers absorption lines at one shot without overlapping effect and performing minimal measuring time of few microseconds.

Exhaled breath analysis is a rapidly developing field of noninvasive medical diagnostics. To date, more than 800 substances have been identified among the products of physiological and biochemical processes in the human body. Their concentrations reflect the level of homeostasis, as well as the severity of pathologies and diseases [2,3]

The high-resolution THz spectroscopy method shows considerable promise for fast qualitative and quantitative analysis of various substances (metabolites) appeared in human organism including the breath at specific disease (in particular, cancer diseases, diabetes) for diagnostics at earlier stages or monitoring of patient's state. It allows to control efficiency of current treatment.

The application of high-resolution THz spectroscopy method for medicine diagnostics was used for monitoring the variation of the NO concentration at the radiotherapy course (the absence of nitric oxide in exhaled air of healthy people and its appearance in exhaled air of oncopatients with cancer of lung which had radiotherapy are determined at clinical tests); in the diagnostics and monitoring of the inflammations.

The method of detection of acetone in exhaled breath for earlier diabetes diagnostics shows its competitive ability in comparison with other methods. The experiments of detection of exhaled methanol, ethanol and H_2S and also experiments of simultaneous detection of acetone in exhaled breath and urine samples of diabetes patients show considerable promise for determination of metabolites-markers sets in exhaled breath and vapors of biological liquids unambiguously characterizing the diabetes presence. The results of simultaneous measurements of acetone concentrations at exhaled breath and urine samples of the diabetes patients at the frequency of 151646.597 MHz are presented in Fig.1.

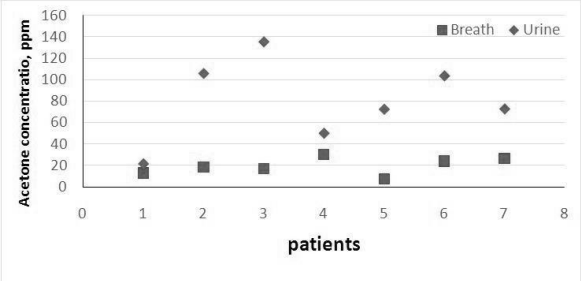

Fig. 1. Simultaneous measurements of acetone concentrations at exhaled breath and urine samples at the frequency of 151646.597 MHz

The possibility of use of terahertz high resolution nonstationary spectroscopy in such agricultural applications as veterinary diagnostics of diseases and pathology states of animals based on analysis of exhaled breath and vapors of biological liquids (urine, saliva); diagnostics of degree of corn mycosis based on analysis of corn odors; monitoring the quality of foodstuff (meat, fish, poultry) based on analysis of its odors shows considerable promise. The investigations of odors of meat and fish samples in fresh and natural decay with using the terahertz high resolution nonstationary spectroscopy methods for were carried out. The results reveal that odor of fresh meat contains ethyl formate, diethyl ether, alanine and glycine, that disappear during natural decomposition process. The latter is characterized by appearing the sulfur compound such as hydrogen sulfide and sulfur dioxide. After that the decaying process is going on with ammonia and nitrogenous organic substances appearance (formamide, ethylamine).In the spoiled fish odor propylene glycol, urethane, hydrogen sulfide, sulfur dioxide and nitriles substances have been found. The high resolution THz spectroscopy as "electronic nose" has been demonstrated to be very promising for food quality analyzing. [4]

Grain	**Substances**
Winter wheat (Nemchinivskaya-17)	Glycolaldehyde ($HCOCH_2OH$)
	Formic acid (HCOOH)
Summer wheat (Sitara)	Formamide (NH_2CHO)

The preliminary results on studying the grain odors composition of winter and summer wheats are presented in the Table. Some chemical substances, which can be results of defeating the grain by necrotrophic pathogens (formamide) or results of seed decomposition at heating, were identified.

Functions of biological molecules (biomolecules) such as DNA and proteins, depend not only on their chemical composition, but also on the spatial structure of the molecules – the so-called configurational and conformational state. The study of configurational and conformational structure of biological molecules is an important task of biology, medicine. Monitoring the conformational transitions occurring during biologically important reactions, such as enzymatic catalysis, will allow a better understanding of the mechanisms of these reactions. Detection of biomolecules with pathological conformations in biological products (blood or cerebrospinal fluid samples) is important for early diagnosis of some diseases, such as prion infections., there are low-frequency molecular vibrations, in which large groups of atoms in a molecule move as a unit (e.g., nucleotide in DNA) in the THz frequency region The frequency of these oscillations depends on the structure of the whole molecule. Oscillation frequencies of hydrogen bonds supporting the structure of biomolecules also lie in the THz frequency range. Therefore, THz absorption spectra contain specific information about the structure and properties of hydrogen bonds. Note that circular dichroism spectra allow one to decipher the structure of molecules and to reconstruct relative positions of atomic groups, but contain no information about hydrogen bonds. The water absorption lines also lie in the THz region. These are dependent on vibrational-rotational transitions and relaxational dielectric losses. Water absorption bands allow to estimate the amount of water in the sample.

Applying methods of THz absorption spectroscopy is difficult due to high complexity of spectra interpretation. There are no detailed spectroscopic databases for polymer molecules in the THz region to date. It is impossible to calculate polymer absorption spectra, taking into account every electron and every nucleus in the molecule. The measurements of THz spectra of DNA and modeling polymers were carried out with using the high resolution THz spectroscopy method [5].

The preliminary investigations of gas-markers in THz frequency range have demonstrated the advantages of the high resolution THz spectroscopy methods for various applications. This approach could be promising to become the compact high precise analytical tool.

This work was carried out in the framework of state targets N 0035-2014-0206 and financially supported by the Russian Foundation for Basic Research (grant N 18-42-520050 r_a_povoljie, N 17-00-00184 KOMFI, N18-52-16017)

References

1. *V. Vaks*, High-Precise Spectrometry of the Terahertz Frequency Range: The Methods, Approaches and Applications// Journal of Infrared, Millimeter and Terahertz Waves. 2012, V. 33, N. 1, P. 43-53..

2. *Stepanov E V* Diodnaya Lazernaya Spektroskopiya i Analiz Molekul-Biomarkerov (Diode Laser Spectroscopy and Analysis of Biomarker Molecules) (Moscow: Fizmatlit, 2009)

3. *V L Vaks, E G Domracheva, E A Sobakinskaya, M B Chernyaeva*. Exhaled breath analysis: physical methods, instruments, and medical diagnostics //Physics-Uspekhi 2014, V. 57, N 7, P. 684 – 701

4. *V.L.Vaks, M.B.Chernyaeva, E.G.Domracheva and S.I.Pripolzin*. Multifrequency laser spectroscopy of biological tissues odors// Proceedings of V International Symposium TOPICAL PROBLEMS OF BIOPHOTONICS, 20 – 24 July, 2015, Nizhny Novgorod, Russia pp.218-219

5. *Vaks, V.L., Semenova, A.V., Guseva, Y.S., Panin, A.N.* Phenomenological model and experimental study of DNA absorption spectra in THz range //Opt. Quant. Electron. 2017, V. 49, N 5, P. 193 (1-24).

High-power Microwaves Against Locusts and Other Harmful Animals

V.E.Zapevalov

Institute of Applied Physics RAS, Nizhny Novgorod, Russia, zapev@appl.sci-nnov.ru

Locusts, acridia - some species of insects of the present locust family (Acrididae), capable of forming large flocks (up to hundreds of millions of individuals) migrating to considerable distances [1-3]. The damage it causes to plants, incomparable. Locusts can destroy all the plants in its path, and its invasion has always been a universal scourge. Innumerable flocks of these insects destroyed the crops, which inevitably led to mass starvation. A feature of biology of the locust is the presence of two phases - single and herd. Herd and single locust phases have significant differences, both in appearance and physiology, and in the nature of behavior. Locusts of a single phase usually have a protective coloration, a well-defined sexual dimorphism, and a low-active solitary lifestyle. Insects of the gregarious phase are colored more brightly and contrastively, adults are more adapted to flight. Locusts in this phase behave much more actively are formed larvae or adults. There is practically no sexual dimorphism in the herd phase. Locust has in its life cycle such stages: eggs, then larvae, the latter – imago (fig.1). The larvae moult 5 times and after the final moult they have wings, the imago stage begins.

The hordes of locusts are able to move at a speed of 15-20 km/h and fly without interruption for up to 20 hours in a row. Huge living clouds of locusts sometimes reach 10 km in width and up to 200 km in length. Two to three days of tailwind is enough for locusts to attack even very remote areas.

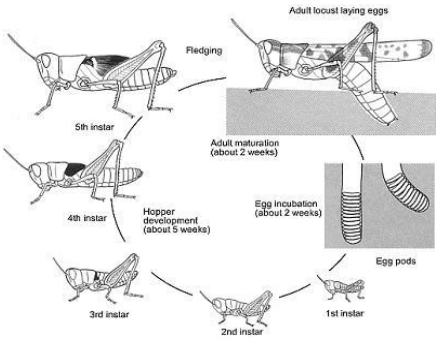

Fig. 1. Locusts: egg capsules; larvae of the 1st- 5th instar; adult insect.

The fight against this evil is conducted worldwide, but almost all used methods have a strong negative impact on the environment [1-3]. Of course, in the late XX -early XXI centuries researchers have the opportunity to obtain fundamentally new data on these insects with the help of molecular-genetic, biochemical and information methods. This especially applies to the mechanisms of the transition from a single phase to a herd and back, migrations of swarms and flocks, and so on. However, these opportunities are often not implemented. This is largely due to the fact that interest in these insects (as well as research funding) falls sharply after the suppression of another outbreak, when the danger for agriculture passes. The ultimate goal in locust control is the use of preventive and proactive methods that disrupt the environment to the least possible extent. This would make agricultural production easier and more secure in the many regions where growing crops is of vital importance to the survival of the local people**.**

In this publication we are going to demonstrate that for control and suppression of locust (and other harmful animals) it is appropriate to use of high-power microwave systems. Important issues are the selection of the frequency range and the required power level for creating mobile microwave complexes. These conditions are determined by technical and economic factors, availability and cost of necessary sources of microwave radiation, transportation (radiation and propagation) of electromagnetic waves, detection of insects and influence on egg capsules, kuligas (larvae), flocks (imago).

The characteristic number of individuals in the migratory flock of locusts is $N \sim 10^7$-10^9 pieces with a density of individuals $n \sim 10^{-3}$-10 m^{-3}. Mass of locust specimen is near ~ 3 g. The characteristic value of biomass in the flock is up to 3000 tons. The time of flock in flight is about ~ 12 hours per day. Locust locating can be remotely conducted by infrared radiation using thermal imagers since the temperature of the clusters is distinctly higher than the underlying surface. Radar and visual methods can be used also.

Important issue is the proper selection of the frequency range and required power levels for exposure to different insects. In the microwave range, the cell membranes become practically short-circuited. Therefore, the electrical properties of suspensions of cells and tissues with high water content are determined by the aqueous, salt and protein content of the intra- and intercellular environment. Fig. 2 shows dielectric properties of water which determine absorption of microwaves (pure water and with salt) as function of wavelength [4, 5].

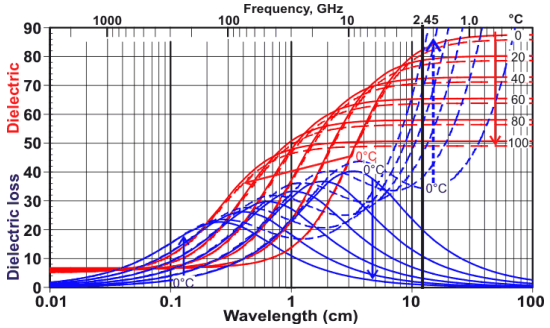

Fig. 2 Absorption of microwaves by water (pure - solid lines, and with salt - dashed lines).

Strong absorption of microwaves by water at the body of insects (pure and mainly with salt as hemolymph) effects on egg-caps, larvae and flocks of imago. In view of the specific structure of insects (fig. 3), effects of microwaves on them are mach stronger than for mammals. All vital locust organs are located close to the surface [1-3], within the skin layer, in contrast to mammals (and in general vertebrates) where 83% of the energy of this radiation is absorbed by the upper layer of the skin.

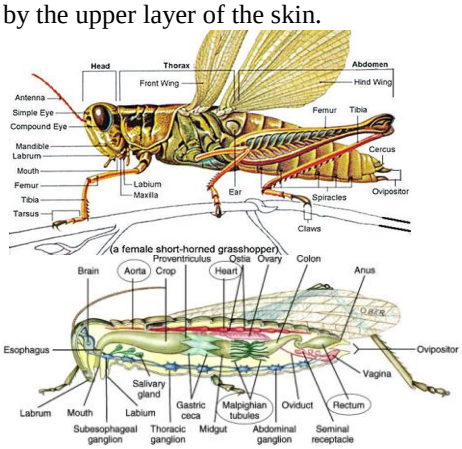

Fig. 3. Scheme of locust and its main organs

It is advisable for effects on eggs and larvae to use a high-efficient magnetrons and gyrotrons [6, 7] at the ISM frequencies (0.915, 2.45, 5.8, 24.125 GHz etc.). Requirements for such type devises for complexes against locust could be discussed. It is reasonable that due to technical and economical reason preferable power level now is 1-3 kW for magnetron (total power of complex near 100 kW) and order of 100 kW for gyrotron.

In adult stage (imago) locust clusters the clear advantages have gyrotron systems of mm range similar non-lethal weapons [8]. Fig. 4 shows vehicle-mounted Active Denial System (ADS). This advanced system uses CPI's VGB-8095 gyrotron to generate a 95 GHz, 100 kW beam which provides a safe but effective deterrent. Similar Chinese system, known as the Poly WB-1, uses millimeter-wave beams (near 30 GHz) to scald targets from up to a kilometer away.

a) b)

Fig. 4. ADS and gyrotron with cryomagnet.

It could be promising to use gyrotron operating at the harmonics of cyclotron frequency **[**7-10**]**. Fig. 5 demonstrates power and efficiency of gyrotron at the 2nd harmonics of cyclotron frequency (the TE_{03}, n=2, $\lambda_0 \approx 12$ *mm*, $f_0 \approx 25$ *GHz*) vs. beam current. Some other acceptable version of gyrotrons for such system described at **[**10]. For those systems RF beam control by phased array antenna it will be practically useful possibility of frequency tuning of RF source [7-8].

There are a lot of other phytophagous and harmful animals of agriculture and forestry in our country and the entire world. The possibility of using similar microwave systems to combat other harmful animals, pests of agriculture and forestry could be developed also.

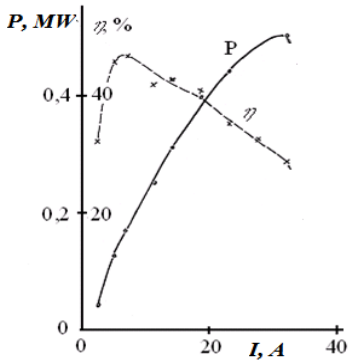

Fig. 5. Power and efficiency of 2nd harmonics gyrotron.

Summary

It is reasonable to use high-power microwaves to control locusts and other harmful animals.
Locust locating can be remotely conducted using thermal imagers because the temperature of the clusters is noticeably higher than the underlying surface.
Due to the peculiarities of the insects structure the microwaves influence for them is much stronger than for mammals.
To effect on he laying of eggs and larvae, it is advisable to use high-efficiency magnetrons and gyrotrons at ISM frequencies. At the adult stage, gyrotron systems, analogous to non-lethal weapons, have clear advantages. The most attractive versions of magnetron and gyrotrons complexes for above mentioned tasks were pointed out.

References

[1] *Resh V.H. (ed.), Carde R.T. (ed.)*. Encyclopedia of Insects. Academic Press. 2003. p.666-669.
[2] *A. Steedman, (ed).* 1990. Locust Handbook (3rd edition). Chatham: Natural Resources Institute. 204 pp.
[3] *B.Uvarov,* 1966. Grasshoppers and locusts, V. I. Cambridge: University Press. 481 pp.
[4] *J. B. Hasted*, Liquid water: Dielectric properties, in Water. A comprehensive treatise, Vol 1, Ed. F. Franks (Plenum Press, New York, 1972) pp. 255-309.
[5] *Sh.E. Tsimring*, Electron beams and microwave vacuum electronics, John Wiley and Sons, Inc., Hoboken, New Jersey, 2007.
[6] *M.Thumm.* State-of-the-Art of High Power Gyro-Devices and Free Electron Masers. *KIT* Scientific Publishing, 2016.
[7] *V.E.Zapevalov*, Evolution of gyrotrons, Radiophysics and Quantum electronics, 2011, v. LIV, №8-9, pp. 559-572.
[8] *V.E.Zapevalov, S.A.Malygin, Sh.E.Tsimring,* Gyrotrons at the second harmonic of the cyclotron frequency. In the book: Gyrotrons, Gorky. IAP, 1980, pp.171-187.
[9] *A.N.Kuftin, V.A.Flyagin, V.K.Lygin, et al*. 5.8-62 GHz cw gyrotrons with warm and permanent magnets for technological application. Proc. of Int. workshop "Strong Microwaves in Plasmas", 1999, N. Novgorod, 2000. pp. 671-676.

The mechanism of the effect of microwave radiation on the parameters of homeostasis in living systems

A.G. Polyakova, A.G. Soloveva, M.V. Presnyakova, V.L. Kuznetsova, P.V. Peretyagin, I.E. Sazonova

Federal State Budgetary Educational Institution of Higher Education «Privolzhsky Research Medical University» of the Ministry of Health of the Russian Federation, Nizhny Novgorod, Russia, ag.polyakova@yandex.ru

One of the actual directions of modern Biomedicine is the study of physical and chemical mechanisms of action of electromagnetic radiation (EMR) on biological systems of various levels of organization [1,2]. An important aspect of the terahertz (THz) range is the presence of molecular spectra of radiation and absorption of the main molecules-metabolites (NO, O2, H2O), as well as large organic molecules: DNA, protein, etc., involved in the pathogenesis of various diseases, regulation of biochemical processes and physiological functions of the body [3,4]. Therefore, of particular interest is the study of the effect of EMR of the THz range on living systems [5-7].

The aim of the work was to experimentally study the effect of low-intensity electromagnetic radiation of the broad-band terahertz range on the metabolic parameters of rat blood in the process of reparative regeneration and the cellular system of hemostasis.

Materials and methods

The experiments were carried out on 15 male Wistar rats weighing 250-300 g. in accordance with the requirements of the Geneva Convention "International Guiding Principles for Biomedical Research Involving Animals" (Geneva, 1990) and blood cells of healthy volunteers (15 people) and 35 patients with burn disease. The impact of EMR was carried out in the direct sound irradiation EMR THz (110-170GHz) from the experimental emitter apparatus "AMFIT" (N.Novgorod).

Animals were divided into 3 equal groups: 1– intact healthy rats, 2 – control – operated animals without any effects, 3 – operated animals with irradiation EMR THz at a dose of 0.12 MJ within the next 7 days (10 minutes 1 time per day). The impact was carried out on the base area of the displaced flap, coinciding with the localization of the skin projection of the center of vegetative regulation. Surgical intervention in 2 and 3 groups of rats and withdrawal from the experiment on day 7 after the operation was carried out under intramuscular anesthesia (Zoletil + Xyla).

Blood stabilized with sodium citrate (1:9) was used for the studies. In plasma and erythrocytes, the activity of free radical oxidation processes was studied using the induced biochemiluminescence method on the biochemiluminometer BHL-06 (N. Novgorod). Chemiluminogenic evaluated total antioxidant activity (TAA) and the ability of a biological object to lipid peroxidation (LPO) with its intensity by the level of malondialdehyde in plasma and hemolysate of washed erythrocytes (1:10), activity of superoxide dismutase (SOD) in hemolysate of washed erythrocytes (1:10) and catalase in erythrocytes by spectrophotometry [8,9]. Glucose and lactate concentrations were measured on a Super GL ambulance device (Germany) in plasma and red blood cells. The activity of lactate dehydrogenase (LDH) was determined on the spectrophotometer Power Wave XS (Bio-Tek, USA).

In the second series of experiments coagulation and platelet units of hemostatic system were studied in 35 patients with thermal trauma and in 15 healthy people in vitro. The effect of EMR on blood cells was carried out in the mode of direct exposure to noise EMR THz (110-170GHz) ranges with exposure 1, 2, 3, 5, 10, 15, 20, 30 and 60 minutes. To assess the plasma level of hemocoagulation system, thromboelastography (TEG in citrated kaolin mode) was used on the TEG 5000 thromboelastograph ("Haemoscope Corporation", USA). Spontaneous platelet aggregation was studied using a laser aggregometer "Biola 230 LA" [6].

Statistical processing was carried out using the program Statistica, version 6.0, using the student and Wilcoxon criteria. Differences were considered statistically significant at $p<0.05$.

Result

In animals of the experimental group under the influence of EMR 110-170 GHz, in the range of which the spectra of nitric oxide and oxygen are located, a pronounced vascular effect was registered, which manifested the smallest zone of ischemia and necrosis in the flap compared to the control group of operated animals (necrosis zone was 23% of the flap area compared to 46% in the control). After the operation, the animals that did not receive radiation were found to have an increase in glucose and total cholesterol, as well as urea concentration in comparison with intact animals. When exposed to EMR 110-110GHz a significant homeostasis effect on biochemical metabolism parameters (total bilirubin, urea, total cholesterol and glucose) was registered).

Under the influence of THz irradiation in animals of the experimental group there was a significant decrease in e intensity of LPO by 14% ($p=0.003$), an increase in blood TAA (8% and 13% respectively) and activation of enzymes of bioradical protection: SOD (30%) and catalase (12%). This inactivates perekisnoe oxidation of lipids and helps to reduce free

radical forms of oxygen, which inhibit the release of catecholamines from the nerve endings and adrenal glands [10]. At the same time, it is possible that one of the mechanisms of EMR THz is the suppression of hyperactivity of one of the most important stress-implementing systems of the sympathoadrenal system.

Thus, in the experimental group of animals, the prevalence of TAA over lipid peroxidation processes was observed, which may indicate the inhibition of the biological oxidation system due to the suppression of reactive oxygen species under the influence of EMR THz. In response to the irradiation of the vegetative regulation center projection, neurohumoral activation of the antioxidant system appears to occur, which blocks the processes of LPO. The revealed change in the direction of LPO processes under irradiation may be due to changes in the structure (conformation) of the cell surface of membrane components due to the weakening of hydrophobic bonds [11].

Exposure to EMR of THz in the noise range 110-170 GHz also contributed to a decrease in lactate concentration in plasma and red blood cells by 34% and 51%, respectively, compared with the control group animals. In parallel, LDH activity increased (by 47% and 23%) compared to the control group.

In addition, it is possible that electromagnetic radiation promotes the use of lactate in carbohydrate metabolism in the formation of 2,3-diphosphoglycerate, the main source of energy in the body.

Analysis of hemostasiological parameters dynamics under the influence of broadband radiation mode revealed activation of plasma hemostasis at 1 and 2 minutes of exposure ($p=0.004$ and 0.02, respectively). Dynamics of changes in coagulation activity in the period from 5 to 60 minutes recorded a gradual decrease in blood coagulation potential, reaching significant differences by 30 minutes compared to the baseline ($p=0.04$). The study of spontaneous aggregation of platelets was demonstrated in the first minutes of exposure to hypercoagulation effect after 30 minutes – hypocoagulation that corresponds to the physiological laws of development of responses of an organism to short the weak and long-strong incentives. A comparative study of the effect of broadband EMR of THz on coagulation and platelet system of hemostasis in patients with thermal injury and healthy people showed no significant differences. Study of the effect of EMR THz on spontaneous platelet aggregation.

Negative effects on the state of tissue blood flow, biochemical and hemostasiological parameters from the studied physical factors were not found.

Conclusion

Exposure to electromagnetic waves of the submillimeter range in the noise mode of radiation plays the role of control signals in the development of biological effects in the body. Based on the results obtained, it follows that low-intensity EMR of THz with a noise range of 110-170GHz in ischemic conditions leads to an increase in the antioxidant status of the blood, as well as inhibition of peroxide States. It is shown that EMR THz noise range of 110-170GHz increases the energy exchange of blood with tissue ischemia. The safety of EMR exposure to THz is evidenced by the absence of a negative side effect on the body of experimental animals.

The results are important for the development of methods of correction of poststress ischemic disorders, which can be successfully used in the process of medical rehabilitation.

Literature

1. Zotova E. A., Malinina Yu. A. et al. Biological effects of millimeter and submillimeter radiation // Izvestiya Samar. science. the centre Grew. Acad. Sciences, 2008. V. 10, No. 2. P. 636–641.
2. Betsky O. V., Kislov V. V., Kozmin A. S., Yaremenko Yu. G. et al. Terahertz waves and their application // Proceedings of the 17th international Crimean conference "Microwave equipment and telecommunication technologies", Ukraine, 2007. V. 2. P. 771–773.
3. Zhang X.C., Jingzhou Xu. Introduction to THz Wave Photonics / Springer, 2010. 248 p.
4. Vaks V. High-Precise Spectrometry of the Terahertz Frequency Range: The Methods, Approaches and Applications // Journal of Infrared, Millimeter and Terahertz Waves, 2012, V. 33, No. 1. P. 43–53.
5. Tsymbal A.A., Kirichuk V.F., Betsky O.V. Reactions of hemostatic system and fibrinolysis to electromagnetic waves of terahertz range // Millimeter waves in biology and medicine, 2011. No.2. P. 23–45.
6. Ponomarenko G.N. Innovative recovery technologies // Resort sheets. Scientific and information journal, 2010. No 5(62). P. 15–18.
7. Kirichuk V.F., Antipova V.F., Tsymbal A. A. et al. Influence of terahertz waves on complex living biological objects /edited by V.F. Kirichuk: Saratov state medical University. Saratov, 2012. 344p.
8. Sibgatullina G.V., Khaertdinova L.R., Gumerova E.A. et al. // Methods for determining the redox status of cultivated plant cells: teaching aid-Kazan: Kazan (Volga region) Federal University, 2011. 61 p.
9. Workshop on free radical oxidation. Educational and methodical manual / F.E. Putilina et al. SPb.:S.-Peterb. State. Univ.of Illinois, 2006. 108 p.
10. Chuyan E.N., Ravaeva M.Y., Nikolskaya V. A. et al.. Scientific notes of Taurida national University. V.I. Vernadsky. Series biology, chemistry 2013, No 26 (65). P. 223.
11. Bajinyan S.A., Meliksetyan A.M., Malakyan M.G. et al.. // Millimeter waves in biology and medicine 2003. No 4. (32). P. 12.

Biomedical applications of terahertz solid immersion microscopy

N. V. Chernomyrdin[1,2,3], A. S. Kucheryavenko[1,3], A. O. Schadko[1], G. A. Komandin[3], V. E. Karasik[1], V. V. Tuchin[4,5,6], and K.I. Zaytsev[1,2,3]

[1] Bauman Moscow State Technical University, Moscow 105005, Russia, chernik-a@yandex.ru
[2] Sechenov First Moscow State Medical University, Moscow 119991, Russia
[3] Prokhorov General Physics Institute of the Russian Academy of Sciences, Moscow 119991, Russia
[4] Saratov State University, Saratov 410012, Russia
[5] Institute of Precision Mechanics and Control of RAS, Saratov 410028, Russia
[6] Tomsk State University, Tomsk 634050, Russia

A number of terahertz (THz) imaging and spectroscopy techniques were proposed for biomedical purposes, i.e. for label-free differentiation of tumors and healthy tissues of different localizations: colon [1,2], breast [3,4], skin [5–7], brain [8,9] etc. Nevertheless, some problems are inherent to THz technology. We can note absence of efficient waveguides for the delivery of THz radiation and limited spatial resolution of THz imaging systems. The problem of low spatial resolution is especially important in biomedical applications of THz imaging as some tissue elements and structures have sub-wavelength dimensions. Several approaches had been already proposed for obtaining sub-wavelength resolution of THz imaging. Among them are near-field scanning-probe imaging [10], THz digital holography or synthetic aperture synthesis [11,12], which however require high-power sources, sensitive detectors or sophisticated computations. Another group of methods utilize effects of electromagnetic field localization in the shadow side of a mesoscale dielectric object, i.e. photonic jet effect [13,14] and solid immersion (SI) phenomenon [15,16]. SI microscopy implies focusing of an electromagnetic wave into the evanescent field volume behind a high-index material. In our work we propose SI microscopy assembly achieving 0,15λ resolution for handling and imaging of biological objects and soft tissues.

Developed SI lens include three optical elements: aspherical lens, forming converging beam with good aberrational correction in paraxial field [17], truncated sphere concentric to converging beam and a moveable plane window for biological tissue depositing. Truncated sphere and window were made of high-refractive index material (HRFZ-Si). Silicon window allows to deposit biological samples on the top of it during the scanning in X-Y directions. Favourable combination of aspherical singlet and HRFZ-Si truncated sphere provide 0,15λ resolution which was estimated theoretically using FDTD (finite-difference time-domain) simulations, and experimentally by means of continuous wave imaging of test object with step-like reflectivity distribution [18]. In order to demonstrate sub-wavelength resolution of SI lens for THz imaging of bioloigical objects and tissues we developed experimental setup based on backward wave oscillator as a continuous wave source of THz radiation and Golay cell coupled with mechanical chopper as a broadband detector.

We applied THz SI microscopy to study several types of biological objects and tissues, namely: leaf blades of such plants as mint [19] or poinsettia, artificially grown 300 μm tissue spheroids [20] and freshly excised human tissues of different localizations. In order to prevent tissue dehydration and i.e. minimize changes in THz properties during the measurements we embedded them into a gelatin slab. Gelatin embedding allows to conserve specimens for THz measurements for a long time after the excision. Fig. 1 demonstrate THz imaging of human breast tissue *ex vivo* obtained for the wavelength λ=500 μm. The specimen is formed by dense fibrous connective tissues with large single fat cells and their groups embedded into it. Though fat cells have sub-wavelength scales according to considered THz wavelength, they are clearly observed on the THz image 1(a).

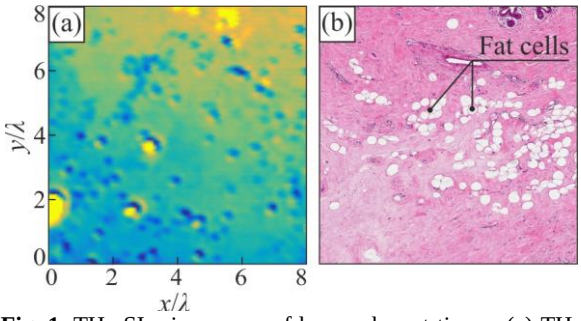

Fig. 1. THz SI microscopy of human breast tissue: (a) THz image observed on λ=500 μm; (b) histological photo.

Described configuration of THz SI microscopy provides the best of the known spatial resolution among SI imaging techniques 0,15λ. It also allows for handling of soft biological tissues during the measurements, thus making THz SI imaging technique a prospective tool for studying sub-wavelength scale inhomogeneity of biological objects.

Acknowledgements

The work was supported by Russian Science Foundation, project # 17-79-20346.

References

1. *Wahaia F. et al.* Terahertz absorption and reflection imaging of carcinoma-affected colon tissues embedded in paraffin // J. Mol. Struct. 2016. V. 1107. P. 214–219.

2. *Reid C.B. et al.* Terahertz pulsed imaging of freshly excised human colonic tissues // Phys. Med. Biol. 2011. V. 56, No. 14. P. 4333–4353.

3. *Fitzgerald A.J. et al.* Terahertz Pulsed Imaging of Human Breast Tumors // Radiology. 2006. V. 239, No. 2. P. 533–540.

4. *Ashworth P.C. et al.* Terahertz pulsed spectroscopy of freshly excised human breast cancer // Opt. Express. 2009. V. 17, No. 15. P. 12444.

5. *Woodward R.M. et al.* Terahertz Pulse Imaging of ex vivo Basal Cell Carcinoma // J. Invest. Dermatol. 2003. Vol. 120, № 1. P. 72–78.

6. *Zaytsev K.I. et al.* In vivo terahertz spectroscopy of pigmentary skin nevi: Pilot study of non-invasive early diagnosis of dysplasia // Appl. Phys. Lett. 2015. V. 106, No. 5. P. 053702.

7. *Zaytsev K.I. et al.* Highly Accurate In Vivo Terahertz Spectroscopy of Healthy Skin: Variation of Refractive Index and Absorption Coefficient along the Human Body // IEEE Trans. Terahertz Sci. Technol. 2015. V. 5, No. 5. P. 817–827.

8. *Meng K. et al.* Terahertz pulsed spectroscopy of paraffin-embedded brain glioma // J. Biomed. Opt. 2014. V. 19, No. 7. P. 077001.

9. *Chernomyrdin N.V. et al.* In vitro terahertz spectroscopy of gelatin-embedded human brain tumors: A pilot study // Progress in Biomedical Optics and Imaging - Proceedings of SPIE. 2018. V. 10716.

10. *Adam A.J.L.* Review of Near-Field Terahertz Measurement Methods and Their Applications // J. Infrared, Millimeter, Terahertz Waves. 2011. V. 32, No. 8–9. P. 976–1019.

11. *Zhang Y. et al.* Terahertz digital holography // Strain. 2008. V. 44, No. 5. P. 380–385.

12. *McClatchey K., Reiten M.T., Cheville R.A.* Time resolved synthetic aperture terahertz impulse imaging // Appl. Phys. Lett. 2001. V. 79, No. 27. P. 4485–4487.

13. *Nguyen Pham H.H. et al.* Asymmetric phase anomaly of terajet generated from dielectric cube under oblique illumination // Appl. Phys. Lett. 2017. V. 110, No. 20. P. 201105.

14. *Minin I.V., Minin O.V.* Terahertz artificial dielectric cuboid lens on substrate for super-resolution images // Opt. Quantum Electron. 2017. V. 49, No. 10.

15. *Mansfield S.M., Kino G.S.* Solid immersion microscope // Appl. Phys. Lett. 1990. V. 57, No.24. P. 2615–2616.

16. *Chernomyrdin N. V. et al.* Solid immersion terahertz imaging with sub-wavelength resolution // Appl. Phys. Lett. 2017. V. 110, No. 22. P. 221109.

17. *Chernomyrdin N.V. et al.* Wide-aperture aspherical lens for high-resolution terahertz imaging // Rev. Sci. Instrum. 2017. V. 88, No. 1. P. 014703.

18. *Chernomyrdin N. V. et al.* Reflection-mode continuous-wave 0.15 λ -resolution terahertz solid immersion microscopy of soft biological tissues // Appl. Phys. Lett. 2018. V. 113, No. 11. P. 111102.

19. *Chernomyrdin N.V. et al.* Terahertz solid immersion microscopy for sub-wavelength-resolution imaging of biological objects and tissues // Progress in Biomedical Optics and Imaging - Proceedings of SPIE. 2018. V. 10716.

20. *Chernomyrdin N. V. et al.* A potential of terahertz solid immersion microscopy for visualizing sub-wavelength-scale tissue spheroids // Proceedings of SPIE. 2018. V. 10677, No. 106771Y.

Intraoperative diagnosis of malignant brain gliomas using terahertz pulsed spectroscopy and optical coherence tomography

K.I. Zaytsev[1,2,*], I.N. Dolganova[2,3], N.V. Chernomyrdin[1,2], G.A. Komandin[1], M.A. Schcedrina[4], S.-I.T. Beshplav[5], S.A. Goryaynov[5], V.E. Karasik[2], I.V. Reshetov[4], A.A. Potapov[5], and V.V. Tuchin[6,7,8]

[1]Prokhorov General Physics Institute of the Russian Academy of Sciences, Moscow 119991, Russia;
[2]Bauman Moscow State Technical University, Moscow 105005, Russia;
[3]Institute of Solid State Physics of the Russian Academy of Sciences, Chernogolovka 142432, Russia;
[4]Sechenov University, Moscow 119991, Russia;
[5]Burdenko Neurosurgery Institute, Moscow 125047, Russia;
[6]Saratov State University, Saratov 410012, Russia, Russia;
[7]Tomsk State University, Tomsk, 634050;
[8]Institute of Precision Mechanics and Control of the Russian Academy of Sciences, Saratov 410012, Russia
*E-mail: kirzay@gmail.com

An intraoperative diagnosis of malignant brain gliomas remains a challenging problem of modern neurosurgery [1]. A complete resection of glioma is the most important factor, determining an efficiency of its treatment [2]; while an incomplete resection, caused by inaccurate detection of the tumor margins, increases a probability of its recurrence. The existing methods of the intraoperative neurodiagnosis of tumors are plagued with limited sensitivity and specificity, some of them remains laborious, time-consuming and/or rather expensive. Therefore, development of novel methods for the intraoperative diagnosis of gliomas relying on modern instruments of medical spectroscopy and imaging is a topical problem of medicine, physics, and engineering [3,4].

In our research, we studied a potential of terahertz (THz) pulsed spectroscopy (TPS) [5–9] and optical coherence tomography (OCT) [10–12] in the intraoperative diagnosis of brain tumors, with a strong emphasize on brain gliomas.

First, we performed *in vitro* THz spectroscopy of human brain gliomas of different grade. In order to fix tissues for the THz measurements, we applied the gelatin embedding, which allows to preserve tissues from hydration/dehydration; thus, sustaining the THz dielectric response of tissues unaltered for a long time after the surgery. We applied the laboratory TPS setup to study *in vitro* the refractive index and the amplitude absorption coefficient of intact tissues and gliomas. We observed significant differences between the THz characteristics of normal and pathological tissues of the brain [13]. This highlights a potential of THz technology in the label-free intraoperative diagnosis of brain tumors. Particularly, THz imaging and microscopy [14] can be applied for the intraoperative detection of the tumor margins in order to ensure its gross-total resection. Furthermore, the single-point THz spectroscopy and reflectometry could be integrated into modern neuroprobes, which are based on sapphire shaped crystals and yields combining the THz waveguiding [16,17] with diagnosis, aspiration and laser coagulation of brain tissues [18–20].

Second, we studied intact tissues and gliomas of the brain using OCT. For each tissue class, we analyzed a slope of the OCT signal in a depth. This slope reveals statistical difference between healthy and pathological tissues of the brain [10], which could be further emphasized using modern wavelet-domain denoising of OCT data [12]. Thus, the results of our study showcase a potential of OCT in intraoperative neurodiagnosis of brain gliomas.

Thereby, this work yields preliminary analysis (feasibility test), which aims to objectively uncover strengths and weaknesses of TPS and OCT from the viewpoint of their use in intraoperative diagnosis of human brain tumors before committing to a full-blown study involving measurements and analysis of a large amount of tissue sample, both *ex vivo* and *in vivo*.

This work was supported by the Russian Foundation for Basic Research (RFBR), Projects # 18-38-00504 and 18-38-00853.

References

1. *Ostrom, Q.T., Gittleman, H., Xu, J., Kromer, C., Wolinsky, Y., Kruchko, C., Barnholtz-Sloan, J.S.,* CBTRUS Statistical Report: Primary Brain and Other Central Nervous System Tumors Diagnosed in the United States in 2009-2013 // Neuro-Oncology, 2016, V.18, No.5, P.1–75.

2. *Phuphanich, S., Ferrall, S., Greenberg,* H., Long-term survival in malignant glioma. Prognostic factors // The Journal of the Florida Medical Association, 1993, V.80, P. 181–184.

3. *Pustogarov, N., Panteleev, D., Goryaynov, S.A., Ryabova, A.V., Rybalkina, E.Y., Revishchin, A., Potapov, A.A., Pavlova, G.,* Hiding in the Shadows: CPOX Expression and 5-ALA Induced Fluorescence in Human Glioma Cells // Molecular Neurobiology, 2017, V.54., No.7, P.5699–5708.

4. *Potapov, A.A., Goryaynov, S.A., Okhlopkov, V.A., Shishkina, L.V., Loschenov, V.B., Savelieva, T.A., Golbin, D.A., Chumakova, A.P., Goldberg, M.F., Spallone, A., Varyukhina, M.D.,* Laser biospectroscopy and 5-ALA fluorescence navigation as a helpful tool in the meningioma resection // Neurosurgical Review, 2016, V.39, No.3, P.437–447.

5. *Zaytsev, K.I., Kudrin, K.G., Karasik, V.E, Reshetov, I.V., Yurchenko, S.O.,* In vivo terahertz spectroscopy of pigmentary skin nevi: Pilot study of non-invasive early diagnosis of dysplasia // Applied Physics Letters, 2015, V. 106, P. 053702.

6. *Zaytsev, K.I., Gavdush, A.A., Chernomyrdin, N.V., Yurchenko, S.O.,* Highly Accurate in Vivo Terahertz Spectroscopy of Healthy Skin: Variation of Refractive Index and Absorption Coefficient Along the Human Body // IEEE Transactions on Terahertz science and Technology, 2015, V. 5, No.5, P. 817–827.

7. *Zaytsev, K.I., Chernomyrdin, N.V., Kudrin, K.G., Reshetov, I.V., Yurchenko, S.O.,* Terahertz spectroscopy of pigmentary skin nevi in vivo // Optics and Spectroscopy, 2015, V. 119, No.3, P. 404–410.

8. *Reshetov, I., Zaytsev, K., Kudrin, K., Karasik, V., Yurchenko, S., Shcherbina, V.,* Terahertz spectroscopy: Pilot study of non-invasive early diagnosis of dysplasia and melanoma // European Journal of cancer, 2015, V.51, No.3, P. S167.

9. *Zaytsev K.I., Katyba G.M., Kurlov V.N., Shikunova I.A., Karasik V.E., Yurchenko S.O.,* Terahertz Photonic Crystal Waveguides Based on Sapphire Shaped Crystals // IEEE Transactions on Terahertz science and Technology, 2016. V.6, No. 4, P. 576–582.

10. *Dolganova, I.N. Aleksandrova, P.V., Beshplav, S.-I.T, Chernomyrdin, N.V., Dubyanskaya, E.N., Goryaynov, S.A., Kurlov, V.N., Reshetov, I.V., Potapov, A.A., Tuchin, V.V. Zaytsev, K.I.,* Wavelet-domain de-noising of OCT images of human brain malignant glioma // Proceedings of SPIE, 2018, V. 10717, P. 107171X.

11. *Carrasco-Zevallos, O.M., Viehland, C., Keller, B., Draelos, M., Kuo, A.N., Toth, C.A. and Izatt, J.A.,* Review of intraoperative optical coherence tomography: technology and applications // Biomedical Optics Express, 2018, V.8, No.3., P.1607–1637.

12. *Dolganova, I.N., Chernomyrdin, N.V., Aleksandrova, P.V., Beshplav, S.-I.T, Potapov, A.A., Reshetov, I.V., Kurlov, V.N., ., Tuchin, V.V. Zaytsev, K.I.,* Nanoparticle-enabled experimentally trained wavelet-domain denoising method for optical coherence tomography // Journal of Biomedical Optics, 2018, V.23, No.9, P.091406.

13. *Chernomyrdin, V.N., Gavdush; A.A., Beshplav, S.-I.T.,Malakhov, K.M., Kucheryavenko, A.S., Katyba, G.M., Dolganova, I.N., Goryaynov, S.A., Karasik, V.E., Spektor, I.E., Kurlov, V.N., Yurchenko,S.O., Komandin,G.A., Potapov,A.A., Tuchin,V.V., Zaytsev,K.I.,* In vitro terahertz spectroscopy of gelatin-embedded human brain tumors: a pilot study // Proceedings of SPIE, 2018, V. 10716, P. 107160S.

14. *Chernomyrdin, N.V. Kucheryavenko, A.S. Kolontaeva, G.S., Katyba, G.M., Dolganova, I.N., Karalkin, P.A., Ponomarev, D.S., Kurlov, V.N., Reshetov, I.V., Skorobogatiy, M. , Tuchin, V.V., Zaytsev, K.I.,* Reflection-mode continuous-wave 0.15λ-resolution terahertz solid immersion microscopy of soft biological tissues // Applied Physics Letters, 2018, V.113, No. 11, P. 111102,

15. *Katyba, G.M., Zaytsev, K.I., Dolganova, I.N., Shikunova, I.A., Chernomyrdin, N.V., Yurchenko, S.O., Komandin, G.A., Reshotov, I.V., Nesvizhevsky, V.V. and Kurlov, V.N.,* Sapphire shaped crystal for waveguiding, sensing and exposure applications // Progress in Crystal Growth and Characterization of Materials (accepted, 2018).

16. *Zaytsev K.I., Katyba G.M., Kurlov V.N., Shikunova I.A., Karasik V.E., Yurchenko S.O.,* Terahertz photonic crystal waveguides based on sapphire shaped crystals // IEEE Transactions on Terahertz science and Technology, 2016, V.6, No. 4, P. 576–582.

17. *Katyba G.M., Zaytsev K.I., Chernomyrdin N.V. Shikunova I.A., Komandin G.A., Anzin V.B., Lebedev S.P., Spektor I.E., Karasik V.E., Yurchenko S.O., Reshetov I.V., Skorobogatiy M., Kurlov V.N. and Skorobogatiy M.,* Sapphire photonic crystal waveguide for terahertz sensing in aggressive environments // Advanced Optics Materials, 2018, DOI: 10.1002/adom.201800573.

18. *Shikunova I.A., Stryukov D.O., Rossolenko S.N., Kiselev A.M., Kurlov V.N.,* Neurosurgery contact handheld probe based on sapphire shapedcrystal // Journal of Crystal Growth, 2017, V. 457, PP. 265–269.

19. *Shikunova I.A., Zaytsev K.I., Stryukov D.O., Dubyanskaya E.N., Kurlov V.N.,* Neurosurgical sapphire handheld probe forintraoperative optical diagnostics, laser coagulationand aspiration of malignant brain tissue // Proceedings of SPIE, 2017, V. 10411, P. 104110Q

20. *Katyba G.M., Zaytsev K.I., Dolganova I.N., Shikunova I.A., Chernomyrdin N.V., Yurchenko S.O., Komandin G.A., Reshetov I.V., Nesvizhevsky V.V., Kurlov V.N.,* Sapphire shaped crystals for waveguiding, sensing and exposure applications // Progress in Crystal Growth and Characterization of Materials, 2018, accepted.